Palaeodiet reconstruction of Palaeogene rodents from the Shapaja Section (Tarapoto, Peru) with dental microwear textures

Céline Robinet, Myriam Boivin, Gildas Merceron, Adriana M Candela, Rodolfo Salas-Gismondi, Pierre-Olivier Antoine, Laurent Marivaux

Palaeogeography, Palaeoclimatology, Palaeoecology (https://doi.org/10.1016/j.palaeo.2026.113767)

Palaeodiet reconstruction of Palaeogene rodents from the Shapaja Section (Tarapoto, Peru) with dental microwear textures

Céline ROBINET*[a, b], Myriam BOIVIN [c, d], Gildas MERCERON [e], Adriana Magdalena CANDELA [b], Rodolfo SALAS-GISMONDI [f, g], Pierre-Olivier ANTOINE [a]& Laurent MARIVAUX [a]

[a] UMR 5554 ISEM, Univ Montpellier – CNRS – IRD, Place Eugène Bataillon, F-34095 Montpellier Cedex 05, France. cr.robinet@gmail.com (celine.robinet@umontpellier.fr); pierre-olivier.antoine@umontpellier.fr; laurent.marivaux@umontpellier.fr

[b] División Paleontología Vertebrados, Museo de La Plata, CONICET – Universidad Nacional de La Plata, Paseo del Bosque s/n, La Plata, B1900FWA, Argentina. acandela@fcnym.unlp.edu.ar

[c] Grupo de Paleontología de Vertebrados, Instituto de Ecorregiones Andinas (INECOA), CONICET– Universidad Nacional de Jujuy, Avenida Bolivia 1661, CP 4600, San Salvador de Jujuy, Argentina. mboivin@idgym.unju.edu.ar

[d] Instituto de Geología y Minería (IdGyM), Universidad Nacional de Jujuy, Avenida Bolivia 1661, CP 4600, San Salvador de Jujuy, Argentina.

[e] UMR 7262 Laboratoire PALEVOPRIM, CNRS – INEE – Université de Poitiers, Bât. B35, TSA 51106, F-86073 Poitiers Cedex 9, France. gildas.merceron@univ-poitiers.fr

[f] BioGeo Ciencias Lab, Facultad de Ciencias y Filosofía, Laboratorios de Investigación y Desarrollo (LID), Centro de Investigación para el Desarrollo Integral y Sostenible (CIDIS), Universidad Peruana Cayetano Heredia, Avenida Honorio Delgado 430, Lima 31, Peru.rodolfo.salas@upch.pe

[g] Departamento de Paleontología de Vertebrados, Museo de Historia Natural - Universidad Nacional Mayor San Marcos (UNMSM, DPV-MUSM), Avenida Arenales 1256, Lima 14, Peru.

Abstract

Caviomorphs, or Neotropical hystricognaths, are taxonomically and ecologically diverse rodents with varied feeding habits. The earliest occurrence of the group dates back to the end of the Eocene in Peru, but the trophic ecology of these early caviomorphs and its impact on the evolution of the group are poorly understood. To shed light on the ecology of Palaeogene caviomorphs, we applied a method of dental microwear texture analysis (DMTA) to rodent teeth from the Shapaja sedimentary sequence (Tarapoto, San Martín, Peruvian Amazonia). Several fossil-bearing levels were found within this upper Eocene-lower Oligocene section, including an interval marking the Eocene-Oligocene transition (EOT). We compared the dental microwear textures of 119 fossil specimens representing 11 taxa from distinct levels of the Shapaja section with those of a reference set of 858 recent wild caviomorph specimens, divided into 11 dietary categories. Our results indicate different palaeoecologies for Shapaja caviomorphs depending on the levels and ages considered. We find i) taxa with a tendency toward diets composed of soft elements and ii) other taxa including harder or more abrasive materials. This indicates a variety of resources available in the environment as well as distinct dietary strategies among the rodents studied. This disparity in feeding behaviour persisted throughout the Eocene part of the section, as well as in the lowermost Oligocene levels studied. In contrast, a trend toward a generalist hard-element-based diet is observed in the four taxa from the most recent (earliest Oligocene) and richest level, which could be a response to a local aridification.

Key words – body mass; caviomorphs; DMTA; Eocene-Oligocene transition; palaeoecology

1. Introduction

Rodents are one of the most diverse mammal groups (Wilson and Reeder 2005; Burgin et al. 2018, 2025). Among them, South American hystricognaths, or caviomorphs, are divided into four superfamilies (e.g., Upham and Patterson 2015; Wilson et al. 2016): the Erethizontoidea (Neotropical arboreal porcupines), the Cavioidea (i.e., pacas, rock cavies, guinea pigs, capybaras, maras, and agouties), the Chinchilloidea (i.e., chinchillas, viscachas, and paracanas), and the Octodontoidea (i.e., rats chinchillas, degus, terrestrial and arboreal spiny rats, hutias, bamboo rats, coypus, and tuco-tucos). Caviomorphs are distributed across the continent, mainly and in abundance at low latitudes and in lowlands, such as those of the Amazon Basin, but also in high-altitude areas, such as the Andes (e.g., Patton et al. 2015; Ojeda et al. 2015; Lacher et al. 2016; Maestri and Patton 2016). Thus, they are found in highly-varied environments, and they occupy numerous and distinct ecological niches (e.g., Patton et al. 2015). This is associated to an astonishing morphological and ecological disparity, with body sizes ranging from about 50g to 65kg (e.g., Álvarez et al. 2017; Boivin et al. 2024), distinct activity patterns and life modes (e.g., Patton et al. 2015; Wilson et al. 2016), and different locomotor behaviours (e.g., Wilson and Geiger 2015). This disparity results from ~40 million years of evolution on the huge South American landmass (Antoine et al. 2012; Upham and Patterson 2015; Boivin et al. 2019a).

Over the past 20 years, the oldest rodent-bearing localities of South America, first Santa Rosa (Frailey and Campbell 2004; Arnal et al. 2020, 2022), then Contamana area (Antoine et al. 2012, 2016; Boivin et al. 2017) and Tarapoto area (Boivin et al. 2018, 2022; Assemat et al. 2019; Antoine et al. 2021), were found in Peruvian Amazonia. Since then, the fossil record of Palaeogene caviomorphs has continued to grow, with several new localities in Western Amazonian being discovered. These materials showed that Amazonia (i.e., proto-Amazonia at that time) played a substantial role in the early evolution of caviomorphs (Frailey and Campbell 2004; Antoine et al. 2012, 2017; Vucetich et al. 2015; Boivin et al. 2019a; Arnal et al. 2020, 2022), including a wide array of stem caviomorphs and early representants of some superfamilies documenting several Palaeogene radiation events (e.g., Boivin et al. 2019a).

The Shapaja section, situated in Peruvian Amazonia (Tarapoto region, San Martín Department, Peru), represents a wealth of successive fossiliferous levels, notably documenting the late Eocene to the early Oligocene timeframe, and including the Eocene-Oligocene transition (EOT; Antoine et al. 2021). The EOT is of particular interest because it was a period of major climate deterioration (i.e., drastic cooling), which was recorded on a global scale. This event substantially constrained and reshaped the structure of aquatic and terrestrial ecosystems worldwide. However, this observation is based almost entirely on palaeontological documentation of ecosystems on northern continents (e.g., Coxall and Pearson 2007; Zanazzi et al. 2007), and remains so far poorly documented on southern continents, particularly at low latitudes in the Neotropics (e.g., Antoine et al. 2021; Buffan et al. 2025). The EOT would be a pivotal time interval for rodents, with the apparition and/or early diversification of the four

caviomorph superfamilies (Boivin et al. 2019a). In this context, the Shapaja section recording the EOT, with mammal communities before, during, and after the EOT, is therefore of paramount importance for documenting this event in this Neotropical region, and better assessing its palaeoecological implications on caviomorph early diversification. The Paleogene fossil-bearing localities of the Shapaja section yielded fossil caviomorphs in varying abundance depending on the level (Boivin et al. 2018, appendix S2; Antoine et al. 2021). These caviomorph remains were studied in detail, and their taxonomic assignment and phylogenetic relationships are well established for most of them (Boivin et al. 2018, 2019a). The fossil material documenting caviomorphs along the Paleogene part of the Shapaja section consists of numerous isolated teeth, revealing a taxonomic richness and a noticeable morphological diversity throughout the section, with the record from small to medium-sized taxa (sensu Boivin et al. 2019a) and brachydont, mesodont, and protohypsodont crown height categories (Boivin et al. 2018). Three caviomorph assemblages were recognized which would show two taxonomic turnovers (i.e., before and after the EOT; Antoine et al. 2021).

Body mass and diet are key factors in the ecology of organisms (e.g., Bowers and Brown 1982; Damuth and MacFadden 1990; McNab 2008), and both can be estimated from isolated teeth. Indeed, the dental microwear on the occlusal enamel surface of molars is directly linked to the physical properties of the last masticated food items (e.g., Ungar et al. 2012; Calandra and Merceron 2016; DeSantis 2016). In particular, dental microwear texture analysis (DMTA), based on the automatic quantification of three-dimensional (3D) surfaces, in this case through a scale-sensitive fractal analysis (Ungar et al. 2003; Scott et al. 2005, 2006), is efficient for detecting inter- and intra-specific variations of diet in extant toothed mammals (e.g., Merceron et al. 2010; Scott 2012; Scott et al. 2012; Kaiser et al. 2016; Berlioz et al. 2017; Percher et al. 2018; Merceron et al. 2021). This method also proved to be a valuable proxy for diet reconstruction in fossil toothed mammals (e.g., Ungar et al. 2012; Berlioz et al. 2018; Merceron et al. 2018; Hullot et al. 2025). Undertaking DTMA is now possible for caviomorph rodents as several studies identified and described the relationships between dental microwear textures (DMTs) and dietary behaviours and preferences in extant species of the group. This relationship was enlightened both experimentally (Winkler et al. 2019, 2020) and on natural populations at local (Robinet et al. 2020, 2022), regional, and global scales (Robinet 2023; Robinet et al. 2025, in press).

By comparing the DMTs of the Palaeogene caviomorphs from the Shapaja section to the established referential on their extant representatives (Robinet 2023; Robinet et al. 2025, in press), we here estimate the dietary preferences of those extinct taxa. We further attempt to infer these preferences (i) for each studied level and then (ii) through time, with a specific focus on the EOT and the global environmental changes associated with it (e.g., Prothero and Berggren 1992; Coxall and Pearson 2007; Liu et al. 2009).

2. Materials

We studied 119 specimens of fossil caviomorphs representing 11 taxa (Table 1), previously described by Boivin et al. (2018), coming from five fossil-bearing localities (TAR-01, TAR-13, TAR-20, TAR-21, and TAR-22) along a short stratigraphic section documenting the Upper Pozo (shale) Member (Fig. 1; Hermoza et al. 2005; Roddaz et al. 2010; Antoine et al. 2021). The section is located about 12 km southeast of the city of Tarapoto (Department of San Martín, Peru), near the village of Shapaja, and at the junction of the Mayo River and the Huallaga River (Fig. 1; 6° 34′ 59″ S -76° 16′ 53.15″ W; Boivin et al. 2018; Antoine et al. 2021). In stratigraphic order, TAR-20 is considered to be late Eocene in age, TAR-21 is latest Eocene in age, just before or within the Eocene/Oligocene transition, TAR-22 and TAR-13 both early Oligocene in age, and TAR-01 represents the youngest level, also early Oligocene in age (Fig. 1; see also figure 6 in Antoine et al. 2021). Other rodent-bearing localities of TAR-74 and TAR-72, both late Eocene in age, could not be studied here due to the limited number of specimens and/or the insufficient preservation of their occlusal wear facet (for illustrations, see Antoine et al. 2021).

The studied specimens were unearthed along several field campaigns (2012–2017) by the joint teams of the ISEM lab (Montpellier, France) and the *Departamento de Paleontología de Vertebrados* of the *Museo de Historia Natural* (Lima, Peru). Fossils were recovered by wet acid-free screening method (more than 2000 kg of raw sediment treated; see SI, Antoine et al. 2021). The specimens are curated in the palaeontological collections of the *Museo de Historia Natural of the Universidad Nacional Mayor San Marcos*, in Lima (Peru; Supp. Data 1).

3. Methods

3.1 Body weight estimation

We estimated the body mass of the fossil taxa from measures of their cheek teeth (Boivin et al. 2018) following the protocol proposed by Boivin et al. (2024; Table 2 and Supp. Data 2). A best model set (Boivin et al. 2024, tables 1-3) was first selected depending on the size range each extinct taxon belongs to (Supp. Data 2). Within the best model set selected, we used the equation that corresponds to the best model (i.e., lowest mean of the percent of prediction errors corrected) given the available dental locus for each taxon. When several identical dental loci of different specimens were available for one extinct species, the mean of specimens was used for body mass estimation (see Yapuncich 2018). We calculated the confidence interval (CI; 95%; z-score = 1.96) of each body mass estimation, that corresponds to the range of values that likely contains the true mean response at a given x (i.e., locus measurement), with the function '*predict*' of the "caper" package v.1.0.3 (Orme et al. 2023) in R environment v.4.3.1 (R Core Team 2023). The CI limits were retransformed back and then multiplied by the corresponding

ratio estimator (RE; Snowdon 1991; Table 2). As the CI cannot be obtained for a PGLS model (i.e., *Eoincamys valverdei* from TAR-13; Garland and Ives 2000), we calculated intervals considering the CI of each equation parameter (Supp. Data 2).

3.2 Dental Microwear Texture Analysis (DMTA)

To assess the diet of the fossil caviomorphs, we studied the mesiolingual region of the protocone on upper molars and the distolabial region of the protoconid on lower molars (Fig. 2), with a preference for the two first molars when the material was abundant. We excluded any teeth that were poorly preserved, as well as any specimens showing signs of alteration (perimortem or taphonomic). The DMT of the extinct caviomorph taxa from Shapaja has been analysed in light of the microwear patterns assembled for extant caviomorph taxa, obtained on first upper molars, and for which taxa the feeding habits and some other life history traits are known, as detailed in Robinet (2023) and Robinet et al. (2025, in press). The extant dataset is composed of 858 specimens representing 80 species of caviomorph rodents, grouped in 11 dietary categories (Table 3, Fig. 3A) based on the physical properties of items included in their diet and their feeding behaviour (for a more detailed presentation of the extant reference dataset, see Robinet 2023; Robinet et al. 2025, in press).

We followed the protocol developed in previous studies (Merceron et al. 2016a) and adapted to caviomorph rodents in Robinet et al. (2020, 2022, 2025, in press) and Robinet (2023). We followed the protocol of Calandra et al. (2022) which aim to control the quality of the acquired and processed 3D data to improve the robustness of further analysis. The area of interest was cleaned twice with cotton swab soaked in acetone or ethanol, and then moulded twice using polyvinylsiloxane (Regular Body President, ref. 6015 - ISO 4823, medium consistency, polyvinylsiloxane addition type; Coltene Whaledent). The dental microwear analyses were conducted on the second mould using the Leica DCM8 confocal profilometer "TRIDENT" profilometer housed at the PALEVOPRIM lab (CNRS, and *Université de Poitiers*). The scans were obtained with white light confocal technology using the 100× objective (Numerical aperture: 0.90; working distance: 0.9 mm; Leica Microsystems). The scans were then pre-treated under Leica Map v. 8.2 (Leica Microsystems) following different steps: the surface was inverted (as scans were produced on negative replicas), non-measured points were replaced by the mean of the neighbouring points, aberrant peaks were removed (see Merceron et al. 2016b), surface was levelled and form removal (polynomial of second degree) was applied (Francisco et al. 2018). We selected a 50×50µm area, the largest area available for the thinnest enamel wear surface (see Robinet et al. 2020), to be used for DMTA Scale-Sensitive Fractal Analysis (Scott et al. 2005, 2006) with the softwares Toothfrax and Sfrax (Surfract Corporation, Norwich, Vermont, EE.UU.).

The parameters studied here are: "complexity" (area-scale fractal complexity; Asfc), which estimates the roughness at a given scale; "anisotropy" (exact proportion of length-scale

anisotropy of relief; epLsar), which measures the orientation concentration of surface roughness; "heterogeneity of complexity" (heterogeneity of area-scale fractal complexity; HAsfc), reflecting the variation of complexity within the studied zone calculated here from 4, 9, and 16 subsurfaces; and "textural fill volume" (Tfv; textural fill volume at 0.2 µm), which is related to the depth and expansion of the marks forming the texture of the surface (for details, see Scott et al. 2006). The DMT parameters values for each studied surface are available in Supplementary Data 1.

Previous studies (Robinet 2023; Robinet et al. 2020, 2022, 2025, in press) show that, in caviomorph rodents, the complexity and the textural fill volume are respectively the two DMT parameters varying the most in between dietary categories. Overall, soft elements consumers tend to be characterized by low complexity and textural fill volume values. Consumers of abrasive elements show DMT with high textural fill volume values associated with high complexity and low anisotropy. Hard element consumers show generally more intermediate and variable DMT parameters values. However, they are still associated with high values of complexity and anisotropy. Heterogeneity of the complexity is generally interpreted as a reflection of the variability in hard and abrasive elements size within the diet.

3.3 Statistics

We conducted all the statistical analyses on R v.3.5.0 (R Core Team 2024).

Five fossil taxa represented by five or more specimens (*Eoincamys* cf. *pascuali*, n=7; *Mayomys confluens*, n=54; *Shapajamys labocensis*, n=13; *Tarapotomys mayoensis*, n=18; *Tarapotomys subandinus*, n=5) allowed for statistical comparison of their DMT parameters between them. We tested the multivariate normality and ran MANOVA with the "MVN" package (Korkmaz et al. 2014). When a Box-Cox transformation (Box and Cox 1964) for multivariate normality was needed, we used the "car" package (Fox et al. 2012) before conducting a MANOVA on DMT parameters to test differences between fossil taxa. As the MANOVA was not significant, no further tests needed to be conducted. However, the MANOVA was significant when testing for difference between upper and lower molars within taxa. Then, to precise MANOVA results, we conducted ANOVAs for each DMT parameter.

To estimate the dietary preferences of the fossil taxa, those same five taxa were compared to the DMT of 858 extant caviomorphs gathered in 11 dietary categories, as described in Robinet (2023) and Robinet et al. (2025, in press). As the data were non parametric, even after a Box-Cox transformation (Box and Cox 1964), a pairwise Wilcoxon test was employed on the non-transformed DMT parameters to determine which ones showed differences between the different dietary categories and the fossil taxa.

Considering the count of specimens per taxa per locality, in addition to this statistical approach, a descriptive approach was employed. Robinet (2023) and Robinet et al. (2025, in

press) performed a PCA on the dataset of 858 specimens of extant caviomorphs and four DMT parameters (complexity, anisotropy, textural fill volume and heterogeneity of complexity calculated on 16 subsurfaces). The two first principal components represented 67% of the variability, and the 11 dietary categories occupied a continuum along those two axes following the physical properties of the elements consumed (Robinet 2023; Robinet et al. 2025, in press; Fig. 3). The fossil taxa from the different levels of the Shapaja section were projected, through the values of their DMT parameters, onto the graphical representation of the two first principal components established on the extant specimens and dietary categories by Robinet (2023) and Robinet et al. (2025, in press; Fig. 3A). This was done in order to estimate their diet through general trends reflecting physical properties of food items (Fig. 3B). Each level of the Shapaja section, except coeval levels TAR-13 and TAR-22 (Antoine et al. 2021), were considered separately (TAR-20 Fig. 4A; TAR-21, Fig. 4B; TAR-13 and TAR-22, Fig. 4C; TAR-01, Fig. 4D).

All the graphs presented in this study were done using the R package "ggplot2" (Wickham 2011) and Inkscape v.0.91 (Inkscape Project 2020).

4. Results

4.1 Estimation of the body mass of the fossil taxa

The estimated body mass for the sampled taxa from the different levels of the Shapaja section and the confidence intervals for those estimates are presented in Table 2 and Figure 5. The estimated body masses reveal the presence of small rodents (i.e., <1 kg; Boivin et al. 2024). They range from 56.1 g for the octodontoid *Selvamys paulus* from TAR-22 to 382.1 g for the stem caviomorph cf. *Tarapotomys* sp. from TAR-13. The estimated body masses of those two taxa are the only ones going beyond (in both directions) those of the Chinchilloidea. Indeed, representatives of the genus *Eoincamys* exhibit body masses ranging from 74.6 g for *Eoincamys parvus* at TAR-21 to 356 g for *Eoincamys valverdei* at TAR-13.

4.2 Inter- and intra-specific variation of Dental Microwear Texture parameters

The mean and standard deviation of the mean were calculated for complexity (Asfc), anisotropy (epLsar), fine textural fill volume (Tfv), and heterogeneity of complexity (HAsfc4, HAsfc9, and HAsfc16), across the analysed taxa (Table 4). Overall, the Shapaja taxa present DMTs characterised by low values of complexity, associated with variable textural fill volumes (low to intermediate; Table 4).

Among the five taxa compared statistically to each other: *Eoincamys* cf. *pascuali* (TAR-01), *Mayomys confluens* (TAR-01), *Shapajamys labocensis* (TAR-01), *Tarapotomys mayoensis* (TAR-

01), and *Tarapotomys subandinus* (TAR-21), no significant difference in DMTs parameters were detected (Supp. Data 3).

4.3 Estimation of the diet of the fossil taxa

Eoincamys cf. *pascuali* from TAR-01 (n=7), displays significantly less complex DMTs than those characterising the categories "fruit-grass", "fruit-insect", "grass-leaf", "grass-root", "grass-seed" and "leaf" (Tables 4 and 6). Qualitatively, when the values of DMTs of *E.* cf. *pascuali* specimens are projected onto the PCA previously established on modern species, the taxon displays intermediate values along PC1 and PC2, which plots it closer to the values observed for the categories "fruit-seed", "insect-seed" and "leaf-seed" (Table 5, Fig. 4D).

Specimens representing *Eoincamys parvus* from TAR-21 (n=1) and TAR-22 (n=4) have values different from each other, which bring them closer to different dietary categories when projected on the PCA established on modern species (Robinet 2023; Robinet et al. 2025, in press; Fig. 3). Specimens from TAR-22 display intermediate values along both PC1 and PC2, closer to those of the "fruit-seed", "leaf-seed", "fruit-insect" and "insect-seed" categories. Qualitatively, they are not close to either the categories "young leaf" and "fruit-leaf", nor the categories "leaf", "grass-leaf" and "grass-root" (Fig. 4C). On the other hand, the more extreme values of the specimen coming from TAR-21, reflected by high values along PC1, indicate a proximity to the "leaf" category (Fig. 4B).

Eoincamys valverdei (n=8) is found across all levels except TAR-01. When projected on the PCA established on modern species graphical representation (Fig. 3), it shows intra-specific variability in the DMT. Indeed, at TAR-20, the only studied specimen displays low values along PC1 and seems closer to the "fruit-leaf" category, while at TAR-13, the values of the two specimens are intermediate along PC1 and closer to the "fruit-seed", "insect-seed" and "fruit-insect" categories (Fig. 4A and 4C). The specimens from TAR-21 (n=4) and TAR-22 (n=1) display low values both along PC1 and PC2, bringing them closer to the "leaf-seed" category, or the "fruit-seed" one, although in its extreme range (Fig. 4B and 4C).

The DMT of *Kichkasteiromys raimondii*, represented by a single specimen, is characterised by intermediate values (Table 4). When those values are projected on the PCA graphical representation established in the extant species (Fig. 3), the specimen has intermediate values along PC1 and higher values along PC2. These values are close to the categories "fruit-seed", "leaf-seed", "insect-seed" and "leaf" (Fig. 4B).

Mayomys confluens (n=54) from TAR-01, differs significantly from all dietary categories except the "fruit-seed", "insect-seed" and "leaf-seed" categories (Table 5), which is consistent with its projection on the PCA established on extant species (Figs. 3 and 4D). DMTs of *M. confluens* differ from the other categories in complexity, anisotropy and textural fill volume. In fact, the DMTs of *M. confluens* are more complex than those of the "young leaf" consumers,

but less complex than those of the “grass-leaf”, “grass-root”, “grass-seed”, "leaf", “fruit-insect” and “fruit-grass” categories, and present higher textural fill volume values than those of the “fruit-insect”, “fruit-leaf”, “grass-leaf” and “young leaf” categories (Table 4). In addition, the DMTs of *M. confluens* are more anisotropic than those of consumers in the “fruit-grass”, “grass-seed”, “grass-root” and “leaf” categories (Tables 4 and 6).

Selvamys paulus is represented by two specimens from TAR-22. The extreme values of *S. paulus* fall outside the categories in the PCA plot (Fig. 4C). However, the DMTs of *S. paulus* are characterized by high values of complexity and textural fill volume (Table 4), which are strongly associated with the consumption of abrasive elements (Robinet et al. 2025, in press) and a high anisotropy (Table 4) which could point toward the inclusion of some hard elements (Robinet et al. 2025, in press).

Shapajamys labocensis (n=13) from TAR-01, has a significantly higher microwear texture complexity than that of consumers from the “young leaf” category, but lower than that of those from the “fruit-insect”, “fruit-grass”, “fruit-grass”, “grass-leaf”, “grass-root”, “grass-seed” and “leaf” categories (Tables 4 and 6). The projection of *S. labocensis* DMT values on the PCA graphical representation established in the extant species (Fig. 3) is consistent with the results of the statistical analyses with overall intermediate values along both PC1 and PC2 (Table 4, Fig. 4D).

Tarapotomys mayoensis (n=18) from TAR-01 is characterised by DMTs that, like *M. confluens*, are significantly more complex than those of the “young leaf” consumers but less complex than those of the “grass-leaf”, “grass-root”, “grass-seed”, ‘leaf’, “fruit-insect” and “fruit-grass” categories (Tables 4 and 6). *Tarapotomys mayoensis* DMTs also present significantly higher textural fill volume values than those of the “fruit-insect”, “fruit-leaf” and “young-leaf” categories (Tables 4 and 6). The projection of *T. mayoensis* DMT values in the PCA graphical representation established in extant caviomorphs (Fig. 3), with overall intermediate values along both PC1 and PC2, is consistent with the results of the statistical analyses (Table 4, Fig. 4D).

Tarapotomys subandinus (n=5) from TAR-21, displays significantly less complex DMTs than consumers of the categories “grass-seed”, “grass-root”, “grass-leaf” and “leaf” (Tables 4 and 6). Qualitatively, when the values of *T. subandinus* DMTs are projected onto the extant dietary categories PCA (Fig. 3), the taxon appears having intermediate values along both PC1 and PC2, bringing it closer to the observed values of the categories “fruit-insect”, “fruit-seed”, “insect-seed” and “leaf-seed”, and less to those of the categories “young-leaf”, “fruit-leaf” and “fruit-grass” (Fig. 4B).

The taxon cf. *Tarapotomys* sp. is documented in TAR-20 by three specimens, and by a single specimen in both TAR-21 and TAR-13. When projected on the PCA graphical representation of extant caviomorph dietary categories (Fig. 3), the DMTs of cf. *Tarapotomys* sp. are slightly distinct in each level. The specimens referred to as cf. *Tarapotomys* sp. from TAR-20 have DMTs values intermediate along both PC1 and PC2, in the range of the “fruit-seed”, “leaf-seed”,

“insect-seed” and “fruit-leaf” categories (Table 4, Fig 4A), meanwhile cf. *Tarapotomys* sp. from TAR-21 has slightly lower values along PC2, close to “fruit-seed”, “leaf-seed” and “insect-seed” categories but not the “fruit-leaf” category (Fig. 4B). At TAR-13, cf. *Tarapotomys* sp. shows distinct values which project it with lower values along PC1 and higher values along PC2, corresponding to the extreme ranges of “fruit-leaf” and “fruit-seed” categories (Table 4, Fig. 4C).

When the DMT values obtained on the single specimen referred to aff. *Tarapotomys* sp. are projected on the PCA established on extant species (Fig. 3), it displays a low position along PC1 and slightly high position along PC2, close to those of species belonging to the "young leaf" and "fruit-leaf" categories (Table 4, Fig. 4B).

5. Discussion

5.1 Overview and representativity

The tooth morphology of the caviomorph taxa from the Shapaja road section shows an important disparity, with the presence of taxa with both low- and high-crowned teeth, as well as a variable number of lophs/lophids, more or less transversely oriented (Table 6; Boivin et al. 2018). Levels corresponding to the latest Eocene or EOT (TAR-21) and early Oligocene (TAR-13, TAR-22, and TAR-01) contain assemblages of taxa with a wide array of occlusal dental patterns (Table 6; Boivin et al. 2018). The range of body masses recorded, from taxa such as *Selvamys paulus* with an estimated body mass of 56.1 g, to cf. *Tarapotomys* sp., with an estimated body mass of 382.1 g (Tables 2 and 6, Fig. 5) is comparable to what is observed in "recent" example of radiation in rodents, like the Sigmodontinae, which radiation is about 3 My old (Brace et al. 2015). It is worth mentioning though that a large tooth fragment (which could not be included to this study) referred as "Caviomorpha indet. 2" was recovered from TAR-01 and hints to the presence of at least one bigger taxon in this level (Antoine et al. 2021). All the levels yield taxa with a disparity of body masses (Table 2, Fig. 5). It is worth mentioning that the fossil species recovered represent only a subset of the real rodent palaeodiversity at that time. Indeed, the Shapaja fossils might represent the result of an accumulation by selective predators, which would therefore limit our sample to taxa being preyed upon (Fernández-Jalvo et al. 2016). Thus, a substantial part of these rodent palaeocommunities may be occulted by biased assemblages, as suggested in other group/localities (e.g., Marivaux et al. 2025). Another very probable source of bias in the fossil record at the Shapaja section is the grain-size effect of the water flow leading to an artificial size-sorting of small to medium-sized species (Antoine et al. 2021). Indeed, if only a specific range of grain size deposits, then, only the taxa which isolated tooth size falls into this range will be accumulated. Many other mammal species, including rodents, particularly larger ones that perhaps composed those communities would be then absent from the fossil record for taphonomic reasons, such as rarity, or because they were not subject to predation.

5.2 Interpretation by level

5.2.1 TAR-20 – Late Eocene

Only two taxa, cf. *Tarapotomys* sp. and *Eoincamys valverdei*, could be studied from TAR-20, which represents one of the oldest levels studied here (Fig. 1, Table 1). The two taxa are of distinct sizes (148.1 g and 309.4 g, respectively; Table 2) and show distinct molar morphology (Boivin et al. 2018). *Eoincamys valverdei* has relatively higher-crowned molars (protohypsodont) relative to those of cf. *Tarapotomys* sp., which has brachydont molars (Table 6; Boivin et al. 2018). This difference is associated with slightly distinct DMTs (Fig. 4A). Thus, a diet composed of soft elements corresponding to the "fruit-leaf" category is estimated for the only specimen of *E. valverdei* that could be studied at TAR-20, whereas a diet that includes a higher proportion of hard elements is envisaged for cf. *Tarapotomys* sp., as it presents similar DMTs to those of the "fruit-leaf" but also “fruit-seed”, "leaf-seed" and "insect-seed" categories (Table 6, Fig. 4A).

A preference for soft dietary items may seem surprising for a taxon with relatively high-crowned molars, as observed in this specimen of *E. valverdei*. This morphology is often associated with the consumption of an abrasive diet that wears away enamel more rapidly than with softer elements (e.g., Janis 1988). However, the study of extant caviomorphs showed that there was a very marked intraspecific variability in some species (Robinet et al. 2022). Thus, the capacity to process abrasive items offered by higher crowned molars might only be exploited in conditions of limited resources to access the so-called “fallback food” (Marshall and Wrangham 2007). As dental microwear is known to be a relatively short-term signal which can be rewritten in the span of weeks (Teaford et al. 2018), such punctual, yet strategic, consumption of abrasive items might not be reflected in the studied specimen of *E. valverdei*’s dental microwear.

5.2.2 TAR 21- Eocene-Oligocene Transition (EOT)

The TAR-21 level documents the latest Eocene or possibly the EOT (Fig. 1; Antoine et al. 2021). Of all the fossil-bearing levels identified along the Shapaja road section, TAR-21 is the most species-rich, with six different rodents, among which those recorded at TAR-20 (Table 1).

The taxonomic diversity observed in TAR-21 is associated with a disparity in both tooth sizes (estimated body-mass range from 74.6 g for *Eoincamys parvus* to 168.8 g for *E. valverdei*; Table 2) and molar crown heights (Table 5). Taxa displaying low-crowned molars (brachydont), such as the erethizontoid *Kichkasteiromys raimondii*, intermediate crown height (mesodont) such as

E. parvus and *Tarapotomys subandinus*, and higher crowns (protohypsodont) such as *E. valverdei* (Table 6), are observed (Boivin et al. 2018). This diversity is associated with distinct dietary tendencies. While the diet of aff. *Tarapotomys* sp. is estimated to be composed of soft items, such as those characterising the "young-leaf" and "fruit-leaf" categories, the DMTs of *E. parvus* indicate the presence of abrasive items in its diet, such as mature dicotyledon leaves (Fig. 4B, Table 6). Between these two trends, the DMTs of the other taxa indicate the presence of hard elements in their diet (Table 6). Within the tendency to consume hard items, *T. subandinus* is closer to the "fruit-seed" and "fruit-insect" categories, cf. *Tarapotomys* sp. is closer to the "fruit-seed", "insect-seed" and "leaf-seed" categories, while *K. raimondii* exhibits DMTs that also share similarities with those of the "leaf" category (Table 6, Fig. 4B). Unlike what is observed in TAR-20, *E. valverdei* recorded in TAR-21 exhibits DMTs similar to those of the "leaf-seed" and "insect-seed" categories and seems to have included more hard elements to its diet (Fig. 4B).

Considering TAR-21 rodents, despite the low number of specimens for each taxon, the variety of diets that can be estimated does not only reflect the availability of various resources but might also reflect a segregation in their exploitation. This would fit with a stratified palaeoenvironment, like the tropical wet forests estimated for TAR-21 (Antoine et al. 2021).

5.2.3 TAR-22 & TAR-13 – Early Oligocene

The stratigraphically coeval levels TAR-22 and TAR-13 are early Oligocene in age and are the lowermost fossil-bearing levels after the EOT of the Shapaja section (Fig. 1). The taxonomic diversity of both levels is lower than that of the underlying level, and the only taxon studied that does not occur in TAR-21 is *Selvamys paulus*, which locally represents the oldest record of Octodontoidea (Antoine et al. 2021).

Despite this low taxonomic diversity, morphological disparity is maintained both in terms of size, ranging from 56.1 g for *S. paulus* to 382 g for cf. *Tarapotomys* sp. (Table 2), and in crown height, including taxa with low-crowned molars, such as *S. paulus* and cf. *Tarapotomys* sp., and taxa with higher-crowned molars, such as *E. valverdei* (Table 6). This diversity is also noticeable in the estimated diets (Table 6, Fig. 4C), with tendencies towards the consumption of soft elements (*E. valverdei* from TAR-22), hard to abrasive elements (*S. paulus*) and hard elements (cf. *Tarapotomys* sp., *E. valverdei* from TAR-13, and *E. parvus*). The diet composed of abrasive elements is less marked than that observed at the lower level (lower anisotropy values in *E. parvus* from TAR-21compared to those of *S. paulus*), and changes in the trends observed in *E. valverdei* and *E. parvus* are noticeable. Indeed, *E. parvus* seems to be a consumer of abrasive elements in TAR-21 turning into a consumer of hard elements in TAR-22, while *E. valverdei*, shifts from being a consumer of hard elements in TAR-21 to a consumer of soft elements in TAR-22 (Table 6, Fig. 4B and 4C).

Despite recording a post-EOT environment (Antoine et al. 2021), characterised at the global scale by cooling and an increase in seasonality associated with drier conditions (e.g., Calvillo-Canadell and Cevallos-Ferriz 2005; Woodcock et al. 2017; Martínez et al. 2021), TAR-13 and TAR-22 appear to still harbour a significant diversity of food resources for rodents. Based on a wealth of associated fossil proxies (animals and plants), Antoine et al. (2021) proposed that local conditions had the effect of maintaining stable environmental conditions for longer than those detected at more global scales.

5.2.4 TAR-01 – Early Oligocene

The TAR-01 fossil-bearing locality, the most recent stratigraphically on the Shapaja road section, testifies a taxonomic turnover (Antoine et al. 2021). We studied four distinct taxa, which make their first appearance in this locality (Boivin et al. 2018; Antoine et al. 2021). The taxa are either medium-sized, around 130 g (Table 2), such as *M. confluens* and *T. mayoensis*, or larger, weighing about 250-290 g (Table 2, Fig. 5), such as *S. labocensis* and *Eoincamys* cf. *pascuali*. Except for *T. mayoensis*, which has mesodont molars with an intermediate crown height, the rodents from TAR-01 all have brachydont dentitions (Table 6). These "incoming" taxa recorded at TAR-01 have feeding habits including hard elements, corresponding to the categories "fruit-seed," "insect-seed" and "leaf-seed" (Table 6, Fig. 4D). This is consistent with the presence at TAR-01 of one or more taxa displaying derived incisor enamel microstructures (transitional type 2-3 and type 3) known to be more crack-resistant (Boivin et al. 2019b). Although the DMTs appear very similar between *S. labocensis* and *Eoincamys* cf. *pascuali*, and between *M. confluens* and *T. mayoensis* (Fig. 4D), no difference in DMTs is significant between the four taxa (Supp. Data 3). This is contrasting with what is observed for TAR-21, TAR-13 and TAR-22, which show a higher diversity of estimated food property trends and estimated diet categories. This might indicate a homogenisation of feeding habits as a result of the ecosystem stabilisation that followed the climate and environmental changes recorded at the EOT (Fig. 6; Antoine et al. 2021). This observation could reflect more opportunistic and generalist behaviours, including varied hard elements, such as different types of seeds and insects.

Plant macro-remains available at TAR-01 suggest the presence of a deciduous forest adapted to prolonged dry periods as a result of more pronounced seasonal patterns (Antoine et al. 2021). Some plants point to the persistence of a stratified forest, although possibly more open, and the proximity of freshwater oxbow lakes (Antoine et al. 2021). Trophic palaeoecology of rodents in TAR-01 matches that of a semi-deciduous forest with marked seasonality, in good agreement with the palaeoenvironment as reconstructed through other proxies (leaves, fruits, and seeds; see Antoine et al. 2021).

5.3 The Shapaja section in its broader context

The EOT marked the most dramatic Cenozoic climate change episode worldwide (e.g., Coxall and Pearson 2007). The global temperatures dropped (e.g., Westerhold et al. 2020), as well as the ocean level (e.g., Miller et al. 2020), and a giant ice sheet started covering the whole Antarctic continent (e.g., Liu et al. 2009), all in a short span of time. The fossil record shows a major mammalian turnover at the time in Europe known as the "*Grande Coupure*" (e.g., Stehlin 1909; Legendre et al. 1991; Weppe et al. 2023). Similar turnovers were identified in Asia (e.g., Meng and McKenna 1998; Sun et al. 2014), North America (e.g., Figueirido et al. 2012; Stucky 2014) and Africa (e.g., de Vries et al. 2021; but see Marivaux et al. 2017, 2024), leading to this geological boundary being described by some authors as the second-most important extinction event in the history of life (Hoyal Cuthill et al. 2020).

However, if higher rates of extinctions are observed in Europe (Weppe et al. 2023), the effect of the EOT on South American mammalian guilds is not that straightforward (Buffan et al. 2025). On one hand, in the centre and southern part of the continent, metatherians (Goin et al. 2010; Abello et al. 2020) and native ungulates (Solórzano et al. 2024) show changes near the EOT, which lead to the term "*Bisagra Patagónica*" (Goin et al. 2010), echoing the European "*Grande Coupure*". These faunal changes may result from the post-EOT climate cooling (Stebbins 1981; Reguero et al. 2010), that triggered in turn a marked vegetational change, from a tropical rainforest to "gymnosperm"-dominated environments (Barreda and Palazzesi 2010). On the other hand, the impact of the EOT seems to have been buffered by the tropical cachet of the northern half of the continent (Wallace hypothesis; Wallace 1878; Kohn et al. 2015; Buffan et al. 2025) and possibly delayed by local, tectonically-driven, -conditions in the case of Shapaja (Antoine et al. 2021). Indeed, at the landmass scale, the major turnover in caviomorphs assemblage composition was detected not at the EOT (Antoine et al. 2021; Buffan et al. 2025) but more recently, between early and late Oligocene (i.e., the Tinguiririan and the Deseadan South American Land Mammal Ages, Boivin et al. 2018; Buffan et al. 2025). Along the studied portion of the Shapaja section, in addition to the turnover described in rodents (Boivin et al. 2018), two distinct assemblages of metatherians were recognised (Fig. 6; Antoine et al. 2021) with the first from TAR-20 to TAR-21 and the second in TAR-01 without clear timing for this turnover (no metatherian were identified in TAR-13 and TAR-22). Outside of the mammals, fish fossils were found in abundance and also show a distinct turnover at TAR-01 (Antoine et al. 2021).

The palaeoenvironment reconstruction along the section, based on the deposits, the fossils of plants, fishes and rays, suggests the presence of a multistratified rainforest with high canopy from the late Eocene to the early Oligocene, with a marked seasonality in precipitations intensifying after the EOT, leading to more open and deciduous forests post-EOT (Fig. 6; Antoine et al. 2021). Nonetheless, several plant species persist through this change in climatic conditions. Our results are consistent with this multistratified environment and a delayed impact of global climate aridification post-EOT shown by the decrease of diet diversity and the

trend towards more generalist dietary habits (Fig. 6), coinciding with the taxonomic turnover (Boivin et al. 2018). They could be further confirmed by investigating other groups (i.e., marsupials) responses to these global changes, and by performing some stable isotopic analysis at the different levels of the Shapaja section.

Acknowledgements

The fossils studied in this work were the result of fieldwork done in the framework of a cooperation agreement between the ISE-M and the MUSM. We are especially grateful to Anne-Lise Charruault (ISE-M) for her invaluable help with the production of the replicas in the *Laboratoire de Paléontologie* of the ISE-M located at the *Université de Montpellier*, and Manon Hullot (Jurassica Museum, Porrentruy, Switzerland) for her contribution to the statistical analysis of dental microwear data. We would like to extend our special thanks to Alicia Álvarez (*Instituto de Ecorregiones Andinas*, Jujuy, Argentina), Michelle Arnal (*Museo de La Plata*, Argentina) and Darin Croft (Case Western Reserve University, Cleveland, USA) for reviewing an earlier version of this work, in its PhD thesis form, and Helder Gomes Rodrigues (*Muséum national d'Histoire naturelle*, Paris, France) and an anonymous reviewer for reviewing this work. Their combined comments, remarks and suggestions greatly improved the quality of the manuscript. Publication ISE-M 2026-074 SUD.

Funding

This work was funded by the international collaboration programs CoopIntEER CNRS-CONICET (n°252540; PI: A. Candela and L. Marivaux) and EcosSud/FonCyT (A14-U01; PI: P.-O. Antoine and F. Pujos), the "*Investissement d'Avenir*" grant (LabEx CEBA, ANR-10-LABX-0025-01, project "EMERGENCE"; PI: L. Marivaux), the National Geographic Society (grant n° 9679-15 to P.-O. Antoine), the ISE-M (IRD "*Projets au Sud*") and the *Laboratoire de Paléontologie* (ISE-M; PI: L. Marivaux). Dental microwear analyses were funded by the "TRIDENT" project of the French National Research Agency (ANR-13-JSV7-0008-01; PI: G. Merceron) and the PALEVOPRIM Lab (CNRS and University of Poitiers, France).

Declaration of competing interests

The authors declare no known competing interests.

Declaration of generative AI and AI-assisted technologies

The authors declare no use of generative AI or AI-assisted technologies in this work.

Data availability statement

The authors attest that all research data related to this work is available in the Supplementary data associated with it.

Author contributions: CRediT

CR: writing – original draft and review and editing, conceptualization, data curation, formal analysis, investigation; MB: methodology, data curation, formal analysis, investigation, writing – review and editing; GM: data curation, funding acquisition; methodology, investigation, resources, writing – review and editing; AMC: funding acquisition, project administration, supervision, writing – review and editing; RSG: resources, writing – review and editing; POA: funding acquisition, writing – review and editing; LM: conceptualization, funding acquisition, project administration, supervision, writing – review and editing

Supplementary data

1. List of the studied specimens and their associated Dental Microwear Texture data
2. Taxa measurements and equations used for body mass estimations
3. Statistical analyses between extinct taxa from the Shapaja section

Bibliography

Abello, M.A., Toledo, N. & Ortiz-Jaureguizar, E. (2020). Evolution of South American Paucituberculata (Metatheria: Marsupialia): adaptive radiation and climate changes at the Eocene-Oligocene boundary. *Historical Biology*, *32*(4), 476–493.

Álvarez, A., Arévalo, R. L. M., & Verzi, D. H. (2017). Diversification patterns and size evolution in caviomorph rodents. *Biological Journal of the Linnean Society, 121*(4), 907–922.

Antoine P.-O., Abello M. A., Adnet S., Altamirano Sierra A. J., Baby P., Billet G., Boivin M., Calderón Y., Candela A., Chabain J., Corfu F., Croft D. A., Ganerød M., Jaramillo C., Klaus S., Marivaux L., Navarrete R. E., Orliac M. J., Parra F., Pérez M. E., Pujos F., Rage J.-C., Ravel A., Robinet C., Roddaz M., Tejada-Lara J. V., Vélez-Juarbe J., Wesselingh F. P., & Salas-Gismondi R. (2016). A 60-million-year Cenozoic history of western Amazonian ecosystems in Contamana, eastern Perú. *Gondwana Research, 31*, 30–59.

Antoine, P.-O., Marivaux, L., Croft, D. A., Billet, G., Ganerød, M., Jaramillo, C., Martin, T., Orliac, M. J., Tejada, J., Altamirano, A. J., Duranthon, F., Fanjat, G., Rousse, S., & Salas-Gismondi, R.

(2012). Middle Eocene rodents from Peruvian Amazonia reveal the pattern and timing of caviomorph origins and biogeography. *Proceedings of the Royal Society B, 279*, 1319–1326.

Antoine, P.-O., Salas-Gismondi, R., Pujos, F., Ganerød, M., & Marivaux, L. (2017). Western Amazonia as a hotspot of mammalian biodiversity throughout the Cenozoic. *Journal of Mammalian Evolution, 24*(1), 5–17.

Antoine, P.-O., Yans, J., Aliaga Castillo, A., Stutz, N., Abello, M. A., Adnet, S., Andriolli Custódio, M., Benites-Palomino, A., Billet, G., Boivin, M., Herrera, F., Jaramillo, C., Mártinez, C., Moreno, F., Navarrete, R. E., Negri, F. R., Parra, F., Pujos, F., Rage, J.-C., Ribeiro, A. M., Robinet, C., Roddaz, M., Tejada-Lara, J. V., Varas-Malca, R., Ventura Santos, R., Salas-Gismondi, R., & Marivaux, L. (2021). Biotic community and landscape changes around the Eocene–Oligocene transition at Shapaja, Peruvian Amazonia: Regional or global drivers? *Global and Planetary Change, 202*, 103512.

Arnal, M., Kramarz, A. G., Vucetich, M. G., Frailey, C. D., & Campbell, K. E. Jr. (2019). New Palaeogene caviomorphs (Rodentia, Hystricognathi) from Santa Rosa, Peru: systematics, biochronology, biogeography and early evolutionary trends. *Papers in Palaeontology, 6*(2), 193–216.

Assemat, A., Boivin, M., Marivaux, L., Pujos, F., Benites-Palomino, A., Salas-Gismondi, R., Tejada-Lara, J. V., Varas-Malca, R. M., Negri, F. R., Ribeiro, A. M., & Antoine, P.-O. (2019). Restes inédits de rongeurs caviomorphes du Paléogène de la région de Juanjui (Amazonie péruvienne): systématique, implications macro-évolutives et biostratigraphiques. *Geodiversitas, 41*(1), 699–730.

Barreda, V., & Palazzesi, L. (2010). Vegetation during the Eocene–Miocene interval in central Patagonia: a context of mammal evolution. In: R. H. Madden, A. A. Carlini, M. G. Vucetich & R. F. Kay (Eds.), *The paleontology of Gran Barranca: evolution and environmental change through the Middle Cenozoic of Patagonia* (pp. 375–382). Cambridge, UK: Cambridge University Press.

Berlioz, E., Azorit, C., Blondel, C., Tellado Ruiz, M. S., & Merceron, G. (2017). Deer in an arid habitat: dental microwear textures track feeding adaptability. *Hystrix, 28*(2), 222–230.

Berlioz, E., Kostopoulos, D. S., Blondel, C., & Merceron, G. (2018). Feeding ecology of *Eucladoceros ctenoides* as a proxy to track regional environmental variations in Europe during the early Pleistocene**.** *Comptesrendus Palevol, 17*(4–5), 320–332.

Boivin, M., Marivaux, L., Pujos, F., Salas-Gismondi, R., Tejada-Lara, J. V., Varasmalca, R. M., & Antoine, P.-O. (2018). Early Oligocene caviomorph rodents from Shapaja, Peruvian Amazonia. *Palaeontographica, Abteilung A: Palaeozoology, Stratigraphy, 311*(1–6), 87–156.

Boivin, M., Marivaux, L., & Antoine, P.-O. (2019a). L'apport du registre paléogène d'Amazonie sur la diversification initiale des Caviomorpha (Hystricognathi, Rodentia) : implications phylogénétiques, macroévolutives et paléobiogéographiques. *Geodiversitas, 41*(1), 143–245.

Boivin, M., Marivaux, L., Salas-Gismondi, R., Vieytes, E. C., & Antoine, P.-O. (2019b). Incisor enamel microstructure of Paleogene caviomorph rodents from Contamana and Shapaja (Peruvian Amazonia). *Journal of Mammalian Evolution*, *26*, 389–406.

Boivin, M., Alvarez, A., Ercoli, M.D., Moyano, S.R., Salgado-Ahumada, J.S., Tejerina, A.M.O., & Cassini, G.H. (2024). Body mass estimation from cheek tooth measurements in extinct caviomorphs (Ctenohystrica, Hystricognathi): the importance of predictor, reference sample and method. *Journal of Mammalian Evolution*, *31*(43), p.35.

Bowers, M. A., & Brown, J. H. (1982). Body size and coexistence in desert rodents: chance or community structure? *Ecology, 63*(2), 391–400.

Box, G. E. P., & Cox, D. R. (1964). An analysis of transformations. *Journal of the Royal Statistical Society, Series B, 26*(2), 211–252.

Brace, S., Turvey, S.T., Weksler, M., Hoogland, M.L.P., Barnes, I., 2015. Unexpected evolutionary diversity in a recently extinct Caribbean mammal radiation. *Proceedings of the Royal Society of London*, B 282, 20142371

Burgin, C. J., Colella, J. P., Kahn, P. L., & Upham, N. S. (2018). How many species of mammals are there? *Journal of Mammalogy, 99*(1), 1–14.

Burgin, C. J., Zijlstra, J. S., Becker, M. A., Handika, H., Alston, J. M., Widness, J., Liphardt, S., Huckaby, D. G., & Upham, N. S. (2025). How many mammal species are there now? Updates and trends in taxonomic, nomenclatural, and geographic knowledge. bioRxiv [Preprint]. Mar3:2025.02.27.640393. doi: 10.1101/2025.02.27.640393.

Calandra, I., & Merceron, G. (2016). Dental microwear texture analysis in mammalian ecology. *Mammal Review, 46*(3), 215–228.

Calandra, I. (2022). A workflow for quality control in surface texture analysis applied to teeth and tools. *Journal of Archaeological Science: Reports*, *46*, 103692.

Calvillo-Canadell, L., & Cevallos-Ferriz, S. R. S. (2005). Diverse assemblage of Eocene and Oligocene leguminosae from Mexico. *International Journal of Plant Sciences*, *166*(4), 671–692.

Coxall, H.K., & Pearson, P.N. (2007). The Eocene–Oligocene Transition. En: Williams, M., Haywood, A.M., Gregory, F.J., Schmidt, D.N. (Eds.), Deep-Time Perspectives on Climate Change: Marrying the Signal from Computer Models and Biological Proxies. The Micropalaeontological Society, Special Publications. The Geological Society, London, pp. 351–387.

Damuth, J., & MacFadden, B. J. (1990). *Body size in mammalian paleobiology: estimation and biological implications*. Cambridge University Press, Cambridge.

DeSantis, L. R. G. (2016). Dental microwear textures: reconstructing diets of fossil mammals. *Surface Topography: Metrology and Properties, 4*(2), 023002.

Fernández-Jalvo, Y., Andrews, P., Denys, C., Sesé, C., Stoetzel, E., Marin-Monfort, D., & Pesquero, D. (2016). Taphonomy for taxonomists: implications of predation in small mammal studies. *Quaternary Science Reviews*, *139*, 138–157.

Figueirido, B., Janis, C. M., Pérez-Claros, J. A., De Renzi, M., & Palmqvist, P. (2012). Cenozoic climate change influences mammalian evolutionary dynamics. *Proceedings of the National Academy of Sciences*, *109*(3), 722–727.

Fox, J., & Weisberg, S. (2012). *An R Companion to Applied Regression*, terceraedicion. Sage Publications, Thousand Oaks, California.

Frailey, C. D., & Campbell, K. E. Jr. (2004). Paleogene rodents from Amazonian Peru: the Santa Rosa local fauna. In: K. E. Jr. Campbell (Ed.), *The Paleogene Mammalian Fauna of Santa Rosa, Amazonian Peru* (pp. 71–130). Natural History Museum of Los Angeles County, Los Angeles, California.

Francisco, A., Blondel, C., Brunetière, N., Ramdarshan, A., & Merceron, G. (2018). Enamel surface topography analysis for diet discrimination. A methodology to enhance and select discriminative parameters. *Surface Topography: Metrology and Properties, 6*(1), 015002.

Garland, Jr, T., & Ives, A. R. (2000). Using the past to predict the present: confidence intervals for regression equations in phylogenetic comparative methods. *The American Naturalist*, *155*(3), 346–364.

Goin, F. J., Abello, M. A., & Chornogubsky, L. (2010). Middle Tertiary marsupials from central Patagonia (early Oligocene of Gran Barranca): understanding South America's Grande Coupure. In: R. H. Madden, A. A. Carlini, M. G. Vucetich & R. F. Kay (Eds.), *The paleontology of Gran Barranca: evolution and environmental change through the Middle Cenozoic of Patagonia* (pp. 69–105). Cambridge, UK: Cambridge University Press.

Hermoza, W., Brusset, S., Baby, P., Gil, W., Roddaz, M., Guerrero, N., & Bolaños, R. (2005). The Huallaga foreland basin evolution: Thrust propagation in a deltaic environment, northern Peruvian Andes. *Journal of South American Earth Sciences*, *19*(1), 21–34.

Hoyal Cuthill, J. F., Guttenberg, N., & Budd, G. E. (2020). Impacts of speciation and extinction measured by an evolutionary decay clock. *Nature*, *588*(7839), 636–641.

Hullot, M., Robinet, C., Vautrin, Q., Tabuce, R., Antoine, P.O., Merceron, G., & Lihoreau, F. (2025). Evolution of dietary preferences of the Lophiodontidae (Mammalia, Perissodactyla) from Southern France. *Palaeogeography, Palaeoclimatology, Palaeoecology*, *675*, 113076.

Inkscape Project. (2020). *Inkscape*. Retrieved from https://inkscape.org

Janis, C. M. (1988). An estimation of tooth volume and hypsodonty indices in ungulate mammals, and the correlation of these factors with dietary preferences. En: D. E. Russell, J.-P. Santoro & D. Sigogneau-Russell (Eds.), *Teeth Revisited: Proceedings of the VIIth International Symposium on Dental Morphology* (pp. 367–387). Éditions du Muséum, Paris.

Kaiser, T. M., Clauss, M., & Schulz-Kornas, E. (2016). A set of hypotheses on tribology of mammalian herbivore teeth. *Surf. Topogr-Metrol*. 4: 14003.

Kohn, M. J., Strömberg, C. A., Madden, R. H., Dunn, R. E., Evans, S., Palacios, A., & Carlini, A. A. (2015). Quasi-static Eocene–Oligocene climate in Patagonia promotes slow faunal evolution and mid-Cenozoic global cooling. *Palaeogeography, Palaeoclimatology, Palaeoecology*, *435*, 24–37.

Korkmaz, S., Göksülük, D., & Zararsiz, G. (2014). MVN: An R package for Assessing Multivariate Normality. *R JOURNAL*, *6*(2), 151–162.

Lacher, T. E. Jr., Murphy, W. J., Rogan, J., Smith, A. T., & Upham, N. S. (2016). Evolution, Phylogeny, Ecology, and Conservation of the Clade Glires: Lagomorpha and Rodentia. In: D. E. Wilson, T. E. Jr. Lacher & R. A. Mittermeier (Eds.), *Handbook of the Mammals of the World: Lagomorphs and Rodents I, Volume 6* (pp. 15–26). Lynx Edicions, Barcelona.

Legendre, S., Crochet, J.Y., Godinot, M., Hartenberger, J.L., Marandat, B., Remy, J.A., Sigé, B., Sudre, J., & Vianey-Liaud, M. (1991). Evolution de la diversité des faunes de mammifères d'Europe occidentale au Paléogène (MP 11 à MP 30). *Bulletin de la Société géologique de France*, *162*(5), 867–874.

Liu, Z., Pagani, M., Zinniker, D., DeConto, R., Huber, M., Brinkhuis, H., Shah, S.R., Leckie, R.M., & Pearson, A. (2009). Global cooling during the Eocene-Oligocene climate transition. *Science*, *323*(5918), 1187–1190.

Maestri, R., & Patterson, B. D. (2016). Patterns of species richness and turnover for the South American rodent fauna. *PloS one*, *11*(3), e0151895.

Marivaux, L., Adnet, S., Benammi, M., Tabuce, R., & Benammi, M. (2017). Anomaluroid rodents from the earliest Oligocene of Dakhla, Morocco, reveal the long-lived and morphologically conservative pattern of the Anomaluridae and Nonanomaluridae during the Tertiary in Africa. *Journal of Systematic Palaeontology*, 15(7), 539–569.

Marivaux, L., Benammi, M., Baidder, L., Saddiqi, O., Adnet, S., Charruault, A.-L., Tabuce, R., Yans, Y., & Benammi, M. (2024). A new primate community from the earliest Oligocene of the Atlantic margin of North-Saharan Africa: systematic, paleobiogeographic and paleoenvironmental implications. *Journal of Human Evolution*, 193, 103548.

Marivaux, L., Charruault, A. L., Adaci, M., Bensalah, M., Mahboubi, M., Mebrouk, F., Ammar, H. K., Essid, E. M., Marzougui, W., Temani, R., & Tabuce, R. (2025). New insights into the diversity of strepsirrhine primates from the late early–early middle Eocene of North Africa (Algeria and Tunisia). *Journal of Human Evolution*, *206*, 103729.

Marshall, A. J., & Wrangham, R. W. (2007). Evolutionary consequences of fallback foods. *International Journal of Primatology*, 28(6), 1219–1235.

Martínez, C., Jaramillo, C., Martínez-Murcia, J., Crepet, W., Cárdenas, A., Escobar, J., Moreno, F., Pardo-Trujillo, A., & Caballero-Rodríguez, D. (2021). Paleoclimatic and paleoecological

reconstruction of a middle to late Eocene South American tropical dry forest. *Global and Planetary Change*, *205*, 103617.

McNab, B. K. (2008). An analysis of the factors that influence the level and scaling of mammalian BMR. *Comparative Biochemistry and Physiology Part A: Molecular & Integrative Physiology*, *151*(1), 5–28.

Meng, J., & McKenna, M.C. (1998). Faunal turnovers of Palaeogene mammals from the Mongolian Plateau. *Nature*, *394*(6691), 364–367.

Merceron, G., Berlioz, E., Vonhof, H., Green, D., Garel, M., & Tütken, T. (2021). Tooth tales told by dental diet proxies: An alpine community of sympatric ruminants as a model to decipher the ecology of fossil fauna. *Palaeogeography, Palaeoclimatology, Palaeoecology*, *562*, 110077.

Merceron, G., Colyn, M., & Geraads, D. (2018). Browsing and non-browsing extant and extinct giraffids: evidence from dental microwear textural analysis. *Palaeogeography, Palaeoclimatology, Palaeoecology*, *505*, 128–139.

Merceron, G., Escarguel, G., Angibault, J.-M., & Verheyden-Tixier, H. (2010). Can dental microwear textures record inter-individual dietary variations? *PLoS One*, *5*(3), e9542.

Merceron, G., Novello, A., & Scott, R. S. (2016b). Paleoenvironments inferred from phytoliths and dental microwear texture analyses of meso-herbivores. *Geobios*, *49*(1–2), 135–146.

Merceron, G., Ramdarshan, A., Blondel, C., Boisserie, J.-R., Brunetiere, N., Francisco, A., Gautier, D., Milhet, X., Novello, A., & Pret, D. (2016a). Untangling the environmental from the dietary: dust does not matter. *Proceedings of the Royal Society B: Biological Sciences*, *283*(1838), 20161032.

Miller, K.G., Browning, J.V., Schmelz, W.J., Kopp, R.E., Mountain, G.S., & Wright, J.D. (2020). Cenozoic sea-level and cryospheric evolution from deep-sea geochemical and continental margin records. *Science advances*, *6*(20), eaaz1346.

Ojeda, R. A., Novillo, A., & Ojeda, A. A. (2015). Large-scale richness patterns, biogeography and ecological diversification in caviomorph rodents. In: A. I. Vassallo & D. Antenucci (Eds.), *Biology of Caviomorph Rodents: Diversity and Evolution* (pp. 121–138). Sociedad Argentina para el Estudio de los Mamíferos, SAREM, Buenos Aires.

Orme, D., Freckleton, R., Thomas, G., Petzoldt, T., Fritz, S., Isaac, N., & Pearse, W. (2023). _caper: Comparative Analyses of Phylogenetics and Evolution in R. R package version 1.0.3, <https://CRAN.R-project.org/package=caper>.

Patton, J. L., Pardiñas, U.F. J., & d'Elía, G. (2015). Mammals of South America. Vol. 2: Rodents. University of Chicago Press, Chicago.

Percher, A. M., Merceron, G., NsiAkoue, G., Galbany, J., Romero, A., & Charpentier, M. J. (2018). Dental microwear textural analysis as an analytical tool to depict individual traits and

reconstruct the diet of a primate. *American Journal of Physical Anthropology*, *165*(1), 123–138.

Prothero, D. R., & Berggren, W. A. (1992). *Eocene-Oligocene Climatic and Biotic Evolution*. Princeton University Press, Princeton.

R Development Core Team (2023). *R: A Language and Environment for Statistical Computing*. v.4.3.1. Vienna: R Foundation for Statistical Computing. www.r-project.Org

R Development Core Team (2024). *R: A Language and Environment for Statistical Computing*. v.3.5.0. Vienna: R Foundation for Statistical Computing. www.r-project.org/

Reguero, M.A., Candela, A.M., & Cassini, G.H. (2010). 24 Hypsodonty and body size in rodent-like notoungulates. In: R. H. Madden, A. A. Carlini, M. G. Vucetich & R. F. Kay (Eds.), *The paleontology of Gran Barranca: evolution and environmental change through the Middle Cenozoic of Patagonia* (pp. 362). Cambridge, UK: Cambridge UniversityPress.

Robinet, C. 2023. *Radiaciones adaptativas y diversidad ecológica de los roedores caviomorfos durante el Paleógeno: caracterización de los componentes ecológicos y de la repartición de los recursos alimentarios (modelos actuales* vs *fósiles)* (Doctoral dissertation, Universidad Nacional de La Plata).

Robinet, C., Merceron, G., Candela, A. M., & Marivaux, L. (2020). Dental microwear texture analysis and diet in caviomorphs (Rodentia) from the Serra do Mar Atlantic forest (Brazil). *Journal of Mammalogy*, *101*(2), 386–402.

Robinet, C., Merceron, G., Catzeflis, F., Candela, A. M., & Marivaux, L. (2022). About inter-and intra-specific variability of dental microwear texture in rodents: Study of two sympatric *Proechimys* (Echimyidae) species from the Cacao locality, French Guiana. *Palaeogeography, Palaeoclimatology, Palaeoecology*, *591*, 110880.

Robinet, C., Merceron, G., Candela, A.M., & Marivaux, L. (in press). Del diente a la dieta: un nuevo modelo de interpretación del microdesgaste dentario en roedores caviomorfos actuales para inferencias paleoecológicas. *Boletim Paleontologia em Destaque.*

Robinet, C., Merceron, G., Candela, A.M., & Marivaux, L. (2025). Del diente a la dieta: modelo de interpretación del microdesgaste dentario en roedores caviomorfos actuales. *SciELO Preprints* https://doi.org/10.1590/SciELOPreprints.14068

Roddaz, M., Hermoza, W., Mora, A., Baby, P., Parra, M., Christophoul, F., Brusset, S., & Espurt, N. (2010). Cenozoic sedimentary evolution of the Amazonian foreland basin system. In: C. Hoorn & F. P. Wesselingh (Eds.), *Amazonia, Landscape and Species Evolution: A Look into the Past* (pp. 61–88). Wiley-Blackwell, Hoboken.

Scott, J.R. (2012). Dental microwear texture analysis of extant African Bovidae. *Mammalia*, *76*(2), 157–174.

Scott, R.S., Teaford, M.F., & Ungar, P.S. (2012). Dental microwear texture and anthropoid diets. *American Journal of Physical Anthropology*, *147*(4), 551–579.

Scott, R. S., Ungar, P. S., Bergstrom, T. S., Brown, C. A., Childs, B. E., Teaford, M. F., & Walker, A. (2006). Dental microwear texture analysis: technical considerations. *Journal of human evolution*, *51*(4), 339–349.

Scott, R. S., Ungar, P. S., Bergstrom, T. S., Brown, C. A., Grine, F. E., Teaford, M. F., & Walker, A. (2005). Dental microwear texture analysis shows within-species diet variability in fossil hominins. *Nature*, *436*(7051), 693–695.

Snowdon, P. (1991). A ratio estimator for bias correction in logarithmic regressions. *Canadian Journal of Forest Research*, *21*(5), 720–724.

Solórzano, A., Núñez-Flores, M., & Rodríguez-Serrano, E. (2024). The rise and fall of notoungulates: How Andean uplift, available land area, competition, and depredation driven its diversification dynamics. *Gondwana Research*, *135*, 116–132.

Stebbins, G.L. (1981). Coevolution of grasses and herbivores. *Annals of the Missouri Botanical Garden*, *68*(1), 75–86.

Stehlin, H.G. (1909). Remarques sur les faunules de mammifères des couches éocènes et oligocènes du Bassin de Paris. *Bull Soc Géol France*, *19*, 488–520.

Stucky, R.K. (1992). Mammalian faunas in North America of Bridgerian to early Arikareean "ages" (Eocene and Oligocene). In: D. R. Prothero & W. A. Berggren (Eds), *Eocene-Oligocene climatic and biotic evolution* (pp464–493). Princeton University Press, Princeton.

Sun, J., Ni, X., Bi, S., Wu, W., Ye, J., Meng, J., & Windley, B.F. (2014). Synchronous turnover of flora, fauna and climate at the Eocene–Oligocene Boundary in Asia. *Scientific reports*, *4*(1), p.7463.

Teaford, M.F., Ungar, P.S., Taylor, A.B., Ross, C.F., & Vinyard, C.J. (2018). In vivo rates of dental microwear formation in laboratory primates fed different food items. *BiosurfaceBiotribology*, 3(4), 166–173.

Ungar, P. S., Brown, C. A., Bergstrom, T. S., & Walker, A. (2003). Quantification of dental microwear by tandem scanning confocal microscopy and scale-sensitive fractal analyses. *Scanning*, *25*(4), 185–193.

Ungar, P. S., Krueger, K. L., Blumenschine, R. J., Njau, J., & Scott, R. S. (2012). Dental microwear texture analysis of hominins recovered by the Olduvai Landscape Paleoanthropology Project, 1995–2007. *Journal of Human Evolution*, *63*(2), 429–437.

Upham, N. S., & Pattterson, B.D. (2015). Phylogeny and evolution of caviomorph rodents: a complete timetree for living genera. In: A. I. Vassallo & D. Antenucci (Eds.), *Biology of Caviomorph Rodents: Diversity and Evolution* (pp. 63–120). Sociedad Argentina para el Estudio de los Mamíferos, SAREM, Buenos Aires.

de Vries, D., Heritage, S., Borths, M.R., Sallam, H.M., & Seiffert, E.R. (2021). Widespread loss of mammalian lineage and dietary diversity in the early Oligocene of Afro-Arabia. *Communications Biology*, *4*(1), 1172.

Vucetich, M. G., Arnal, M., Deschamps, C. M., Perez, M. E., & Vieytes, E.C. (2015). A brief history of caviomorph rodents as told by the fossil record. In: A. I. Vassallo & D. Antenucci (Eds.), *Biology of Caviomorph Rodents: Diversity and Evolution* (pp. 11–62). Sociedad Argentina para el Estudio de los Mamíferos, SAREM, Buenos Aires.

Wallace, A.R. (1878). *Tropical nature, and other essays*. Macmillan and Company.

Weppe, R., Condamine, F.L., Guinot, G., Maugoust, J., & Orliac, M.J. (2023). Drivers of the artiodactyl turnover in insular western Europe at the Eocene–Oligocene Transition. *Proceedings of the National Academy of Sciences*, *120*(52), e2309945120.

Westerhold, T., Marwan, N., Drury, A.J., Liebrand, D., Agnini, C., Anagnostou, E., Barnet, J.S., Bohaty, S.M., De Vleeschouwer, D., Florindo, F., & Frederichs, T. (2020). An astronomically dated record of Earth's climate and its predictability over the last 66 million years. *Science*, *369*(6509), 1383–1387.

Wickham, H. (2011). ggplot2. Wiley Interdiscip. Rev. Comput. Stat. 3, 180–185. https://doi.org/10.1002/wics.147

Wilson, D. E., & Reeder, D. M. (2005). *Mammal Species of the World: a Taxonomic and Geographic Reference, Third Edition*. Johns Hopkins University Press. Baltimore.

Wilson, L. A. B., & Geiger, M. (2015). Diversity and evolution of femoral variation in Ctenohystrica. In: P. G. Cox & L. Hautier (Eds.), *Evolution of the Rodents: Advances in Phylogeny, Functional Morphology and Development* (pp. 510–538). Cambridge University Press, Cambridge.

Wilson, D. E., Lacher, T. E. Jr., & Mittermeier, R. A. (2016). *Handbook of the Mammals of the World: Lagomorphs and Rodents I, Volume 6*. Lynx Edicions, Barcelona.

Winkler, D. E., Schulz-Kornas, E., Kaiser, T. M., De Cuyper, A., Clauss, M., & Tütken, T. (2019). Forage silica and water content control dental surface texture in guinea pigs and provide implications for dietary reconstruction. *Proceedings of the National Academy of Sciences*, *116*(4), 1325–1330.

Winkler, D. E., Tütken, T., Schulz-Kornas, E., Kaiser, T. M., Müller, J., Leichliter, J. Weber, K., Hatt, J.-M., & Clauss, M. (2020). Shape, size, and quantity of ingested external abrasives influence dental microwear texture formation in guinea pigs. *Proceedings of the National Academy of Sciences*, *117*(36), 22264–22273.

Woodcock, D. W., Meyer, H. W., & Prado, Y. (2017). The Piedra Chamana fossil woods (Eocene, Peru). *IAWA Journal*, *38*(3), 313–365.

Yapuncich, G. S. (2018). Alternative methods for calculating percentage prediction error and their implications for predicting body mass in fossil taxa. *Journal of Human Evolution*, *115*, 140–145.

Zanazzi, A., Kohn, M. J., MacFadden, B. J., & Terry, D. O. (2007). Large temperature drop across the Eocene-Oligocene transition in Central North America. *Nature 445*, 639–642.

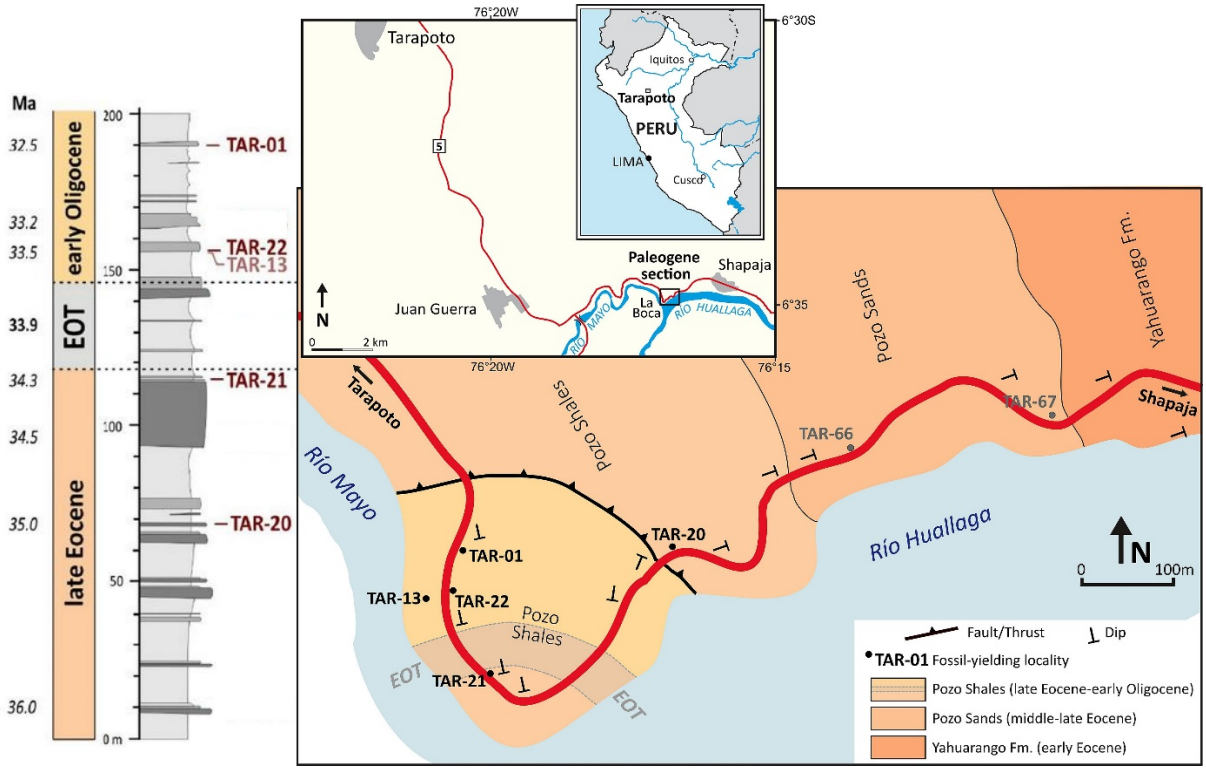

Figure 1: Geographical location of the Shapaja section in Peru, and position of the studied levels in the stratigraphic log of the section. Modified from Antoine et al. (2021).

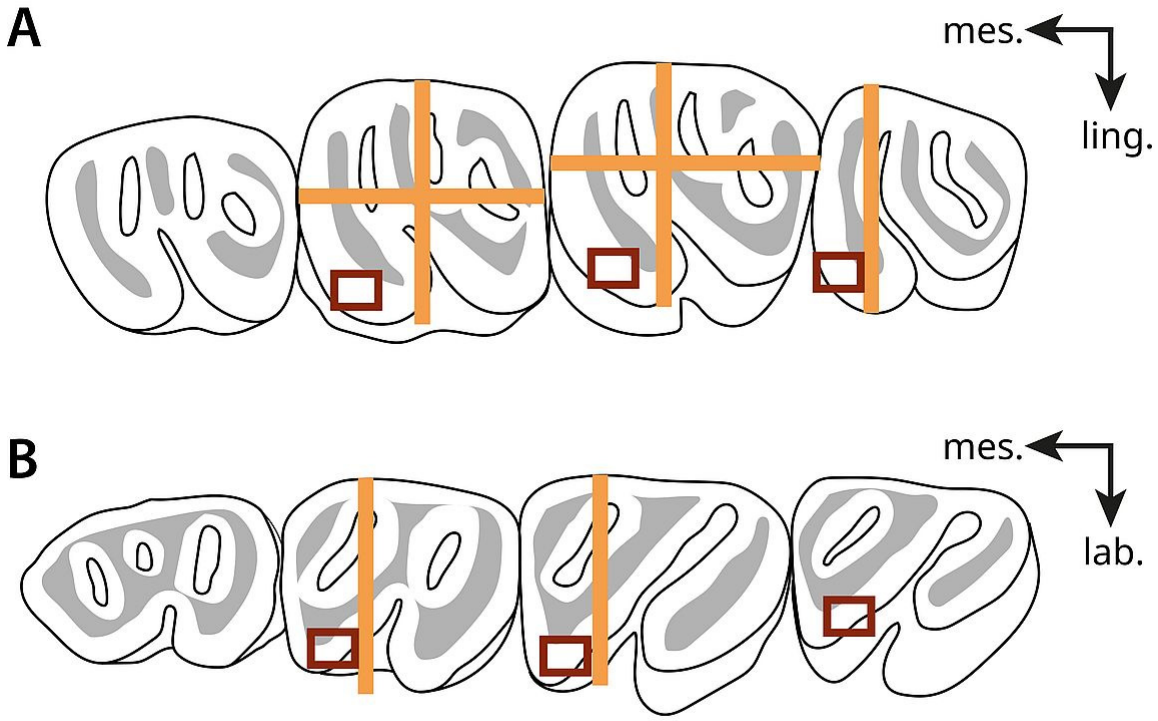

Figure 2: Location of region of interest for the DMTA (dark red rectangles) and measures used for body mass estimations (orange) on upper (A) and lower (B) cheek teeth on fossil taxa. Abbreviation: lab., labial; ling. lingual; mes., mesial.

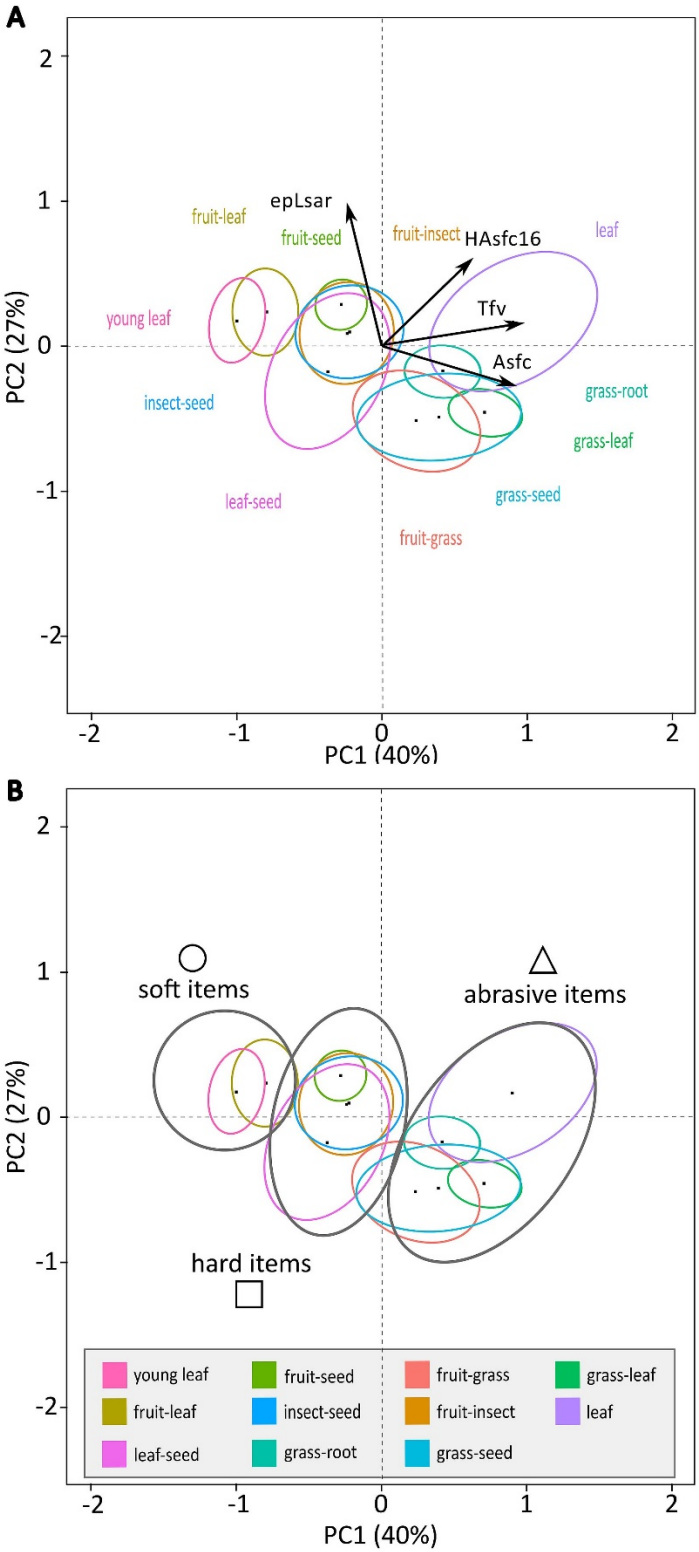

Figure 3: Principal Component Analysis (PCA) of dental microwear texture (DMT) parameters on extant caviomorph taxa (A) from Robinet (2023) and Robinet et al. (2025, in press) and its interpretation regarding general trends of food items physical properties (B) following Robinet (2023) and Robinet et al. (2025, in press). The two first components explain 67% of the variance. Arrows represent the participation to the principal components of the four DMT parameters: Asfc, complexity; epLsar, anisotropy; HAsfc16, heterogeneity of complexity calculated from 16 subsurfaces; Tfv, textural fill volume. The dietary categories are represented by their centroid (black dot) and ellipse of confidence (95%). Circle represents soft elements-based diet, square represents hard elements-based diet, and triangle represents abrasive elements-based diet. Modified from Robinet (2023) and Robinet et al. (2025, in press).

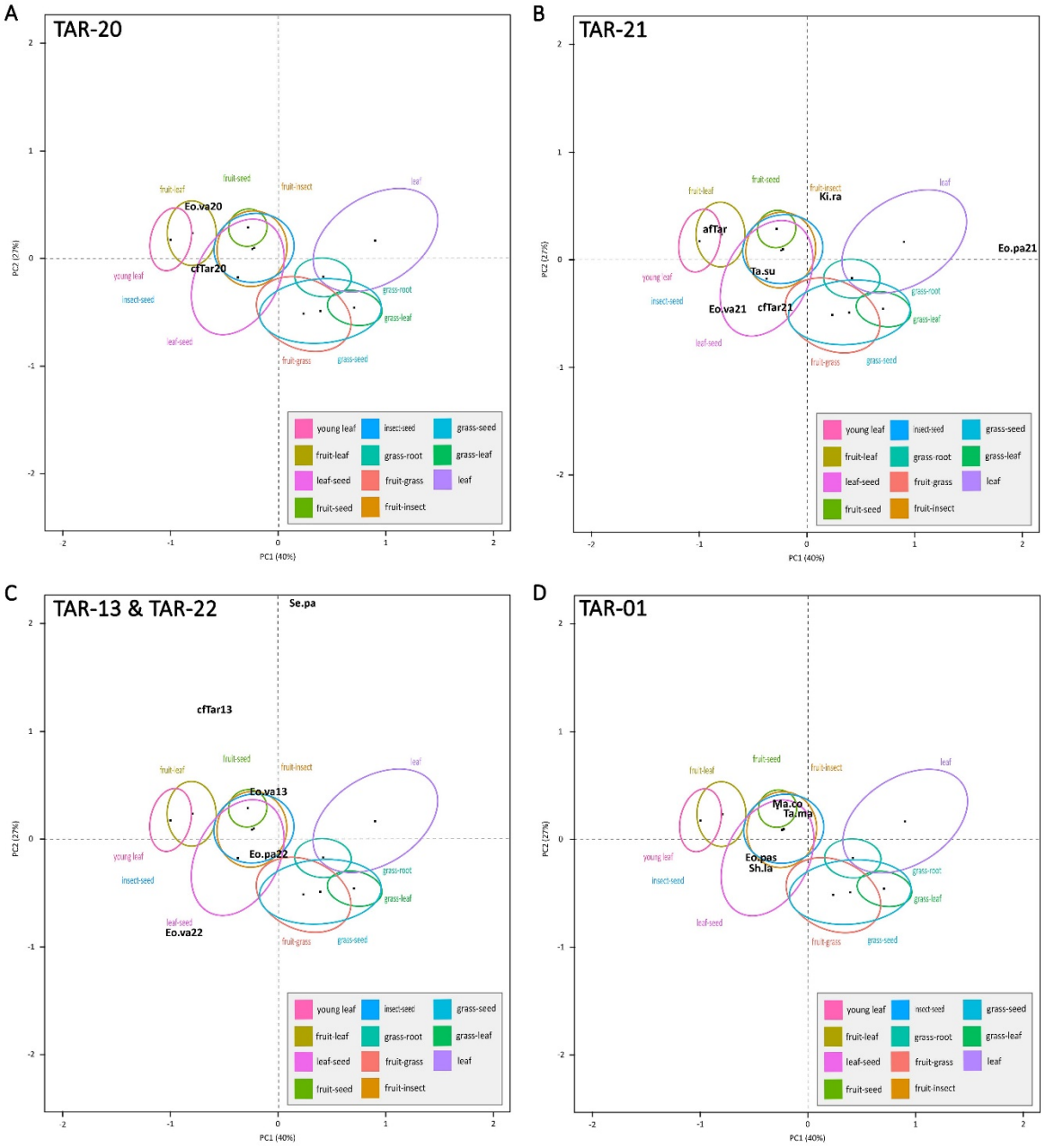

Figure 4: Projection of the fossil taxa DMT parameters values from TAR-20 (A), TAR-21 (B), TAR-13 and TAR-22 (C), and TAR-01 (D) on PC1 and PC2 of the PCA established on extant taxa by Robinet (2023) and Robinet et al. (2025, in press). The 11 dietary categories described in extant taxa are represented by their centroid (black dot) and their ellipse of confidence (95%). The colours follow the legend of Figure 3. The fossil taxa centroids are represented by letters corresponding to their taxonomic affiliation as follows: afTar, aff. *Tarapotomys* sp.; cfTar, cf. *Tarapotomys* sp.; Eo.pa, *Eoincamys parvus*; Eo.pas, *Eoincamys* cf. *pascuali*; Eo.va, *Eoincamys valverdei*; Ki.ra, *Kichkasteiromys raimondii*; Ma.co, *Mayomys confluens*; Se.pa, *Selvamys paulus*; Sh.la, *Shapajamys labocensis*; Ta.ma, *Tarapotomys mayoensis*; Ta.su, *Tarapotomys subandinus*. When a taxon is present in different levels, the number of the level is added to the letters. For example, "Eo.va21" represents the centroid of *Eoincamys valverdei* from TAR-21.

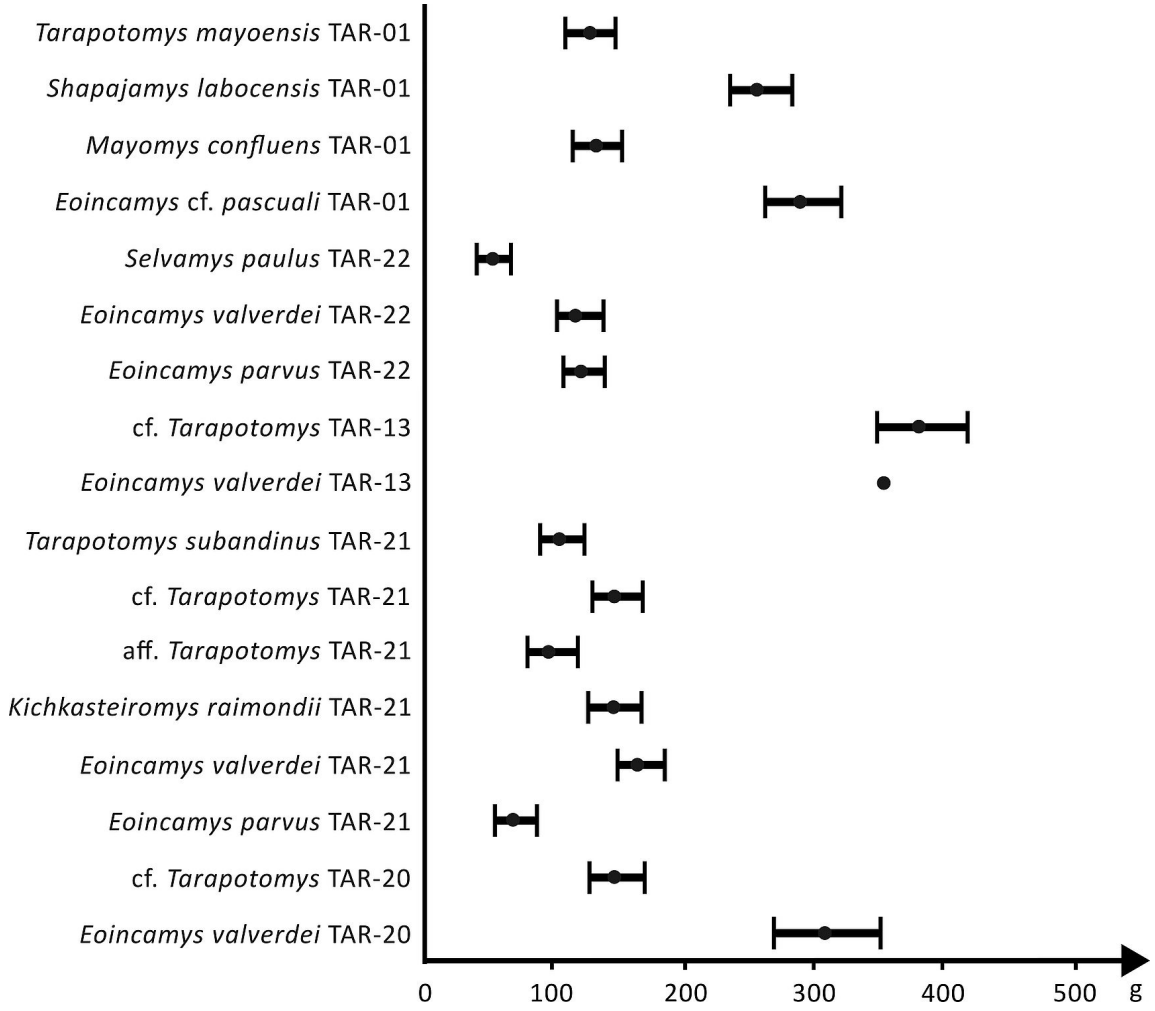

Figure 5: Estimated body mass (g) by taxa by levels of the Shapaja Section. The dots represent the mean and the lines represent the confidence interval of the body mass estimations (95%; z-score = 1.96).

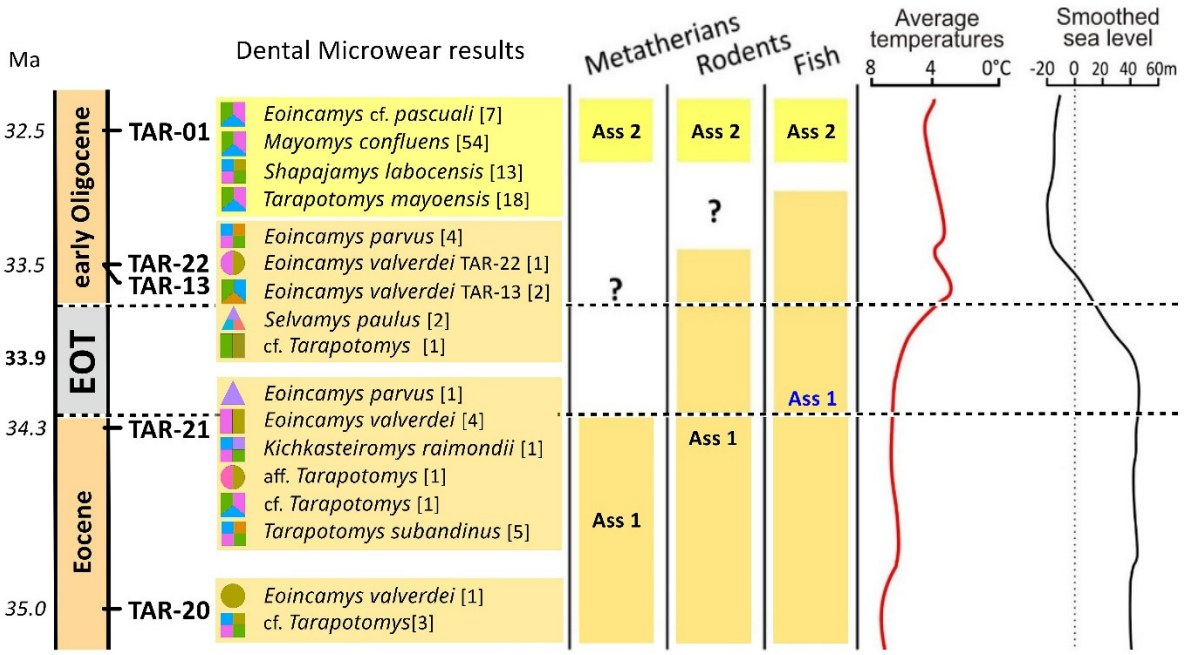

Figure 6: Synthetic chrono-biostratigraphical chart of late Eocene–early Oligocene palaeocommunities from Shapaja, San Martín, Peruvian Amazonia studied here, including the palaeodiet estimations for caviomorph taxa obtained in the present following the shape (circle, soft elements; square, hard elements; triangle; abrasive elements) and colour code given in Figure 3. The number of studied specimens for each taxon is indicated in brackets (cf. Tables 1 and 6). Timeframe based on Vandenberghe et al. (2012) and current chemostratigraphical analyses (Antoine et al. 2021). Ages in italics are approximate and tentative. Assemblages 1–2 derive from Antoine et al. (2021), based on metatherian, rodent, and fish assemblages (selachians + actinopterygians). Blue-typed fish component refers to the marine affinities of Assemblage 1 (mixohaline coastal plain). Palaeotemperature curve (Westerhold et al. 2020) and smoothed sea level curve (Miller et al. 2020) are adapted to match the timeframe of the section. Modified from figure 6 in Antoine et al. (2021). Abbreviation: Ass, Assemblage.

Table 1: List of studied taxa by levels in the Shapaja Section. All taxa were described by Boivin et al. (2018). Supra-generic systematic classification follows Boivin et al. (2019a). The taxa determinate as Caviomorpha correspond to taxa recognized as stem Caviomorpha by Boivin et al. (2019a).

Taxon	N	Supra-generic systematic
TAR-20		
Eoincamys valverdei	1	Chinchilloidea
cf. *Tarapotomys* sp.	3	Caviomorpha
TAR-21		
Eoincamys parvus	1	Chinchilloidea
Eoincamys valverdei	4	Chinchilloidea
Kichkasteiromys raimondii	1	Erethizontoidea
aff. *Tarapotomys* sp.	1	Caviomorpha
cf. *Tarapotomys* sp.	1	Caviomorpha
Tarapotomys subandinus	5	Caviomorpha
TAR-13		
Eoincamys valverdei	2	Chinchilloidea
cf. *Tarapotomys* sp.	1	Caviomorpha
TAR-22		
Eoincamys parvus	4	Chinchilloidea
Eoincamys valverdei	1	Chinchilloidea
Selvamys paulus	2	Octodontoidea
TAR-01		
Eoincamys cf. *pascuali*	7	Chinchilloidea
Mayomys confluens	54	Octochinchilloi
Shapajamys labocensis	13	Caviomorpha
Tarapotomys mayoensis	18	Caviomorpha

Table 2: Estimated body masses following the equations of Boivin et al. (2024) for the fossil taxa by level of the Shapaja section. The dataset refers to the reference sample used by Boivin et al. (2024) to construct the predictive equations: 1.Rodents; 2. rodents + artiodactyls; and 3. rodents + artiodactyls + perissodactyls + hyracoids + lagomorphs. Abbreviations: AM12, occlusal area of M1 or M2; BM, body mass estimations; CI, confidence interval (95%; z-score = 1.96); LM1, maximum anteroposterior length of M1; LM12, maximum anteroposterior length of M1 or M2; LM2, maximum anteroposterior length of M2; WM1, maximum linguolabial width of M1; Wm1, maximum linguolabial width of m1; WM12, maximum linguolabial width of M1 or M2; WM2, maximum linguolabial width of M2; Wm2, maximum linguolabial width of m2; WM3, maximum linguolabial width of M3.

Taxa	Set of best models	Model	Dataset	BM (g)	CI		CI amplitude	Reference
TAR-20								
Eoincamys valverdei	$m_{\%PEc}$*cavio* (Boivin et al. 2024: Table 2)	LM1 + WM1	1	309.4	269.7	355.0	85.3	this work
cf. *Tarapotomys* sp.	$m_{\%PEc}$*cavio* (Boivin et al. 2024: Table 2)	Wm2	1	148.1	130.2	168.5	38.3	this work
TAR-21								
Eoincamys parvus	$m_{\%PEc}$*cavio* (Boivin et al. 2024: Table 2)	LM1 + WM1	1	74.6	63.0	88.3	25.3	this work
Eoincamys valverdei	$m_{\%PEc}$*cavio* (Boivin et al. 2024: Table 2)	LM2	1	168.8	150.7	188.9	38.1	this work
Kichkasteiromys raimondii	$m_{\%PEc}$*cavio* (Boivin et al. 2024: Table 2)	AM12	1	146.7	131.9	163.5	31.6	this work
aff. *Tarapotomys* sp.	$m_{\%PEc}$*cavio* (Boivin et al. 2024: Table 2)	LM12	1	100.8	85.6	118.9	33.4	this work
cf. *Tarapotomys* sp.	$m_{\%PEc}$*cavio* (Boivin et al. 2024: Table 2)	Wm2	1	149.3	131.3	169.8	38.5	this work
Tarapotomys subandinus	$m_{\%PEc}$*cavio* (Boivin et al. 2024: Table 2)	Wm2	1	108.9	94.5	125.6	31.1	this work
TAR-13 & TAR-22								
Eoincamys valverdei TAR-22	$m_{\%PEc}$*cavio* (Boivin et al. 2024: Table 2)	WM3	1	118.3	105.6	132.5	26.8	this work
cf. *Tarapotomys* sp.	$m_{\%PEc}$*cavio* (Boivin et al. 2024: Table 2)	Wm1	1	382.1	348.1	420.2	72.1	this work
Eoincamys parvus	$m_{\%PEc}$*cavio* (Boivin et al. 2024: Table 2)	LM2 + WM2	3	123.6	112.9	135.3	22.4	this work
Eoincamys valverdei TAR-13	$m_{\%PEc}$*cavio* (Boivin et al. 2024: Table 2)	LM12 + WM12	2	356.0	-	-	-	this work
Selvamys paulus	$m_{\%PEc}$*min* (Boivin et al. 2024: Table 3)	LM2 + WM2	1	56.1	46.6	67.4	20.8	this work
TAR-01								
Eoincamys cf. *pascuali*	$m_{\%PEc}$*cavio* (Boivin et al. 2024: Table 2)	Wm2	1	290.0	261.1	322.2	61.1	this work
Mayomys confluens	$m_{\%PEc}$*cavio* (Boivin et al. 2024: Table 2)	Wm2	1	133.9	117.2	153.0	35.8	Boivin et al. 2024: Table 4
Shapajamys labocensis	$m_{\%PEc}$*cavio* (Boivin et al. 2024: Table 2)	Wm2	1	256.6	230.2	286.1	56.0	Boivin et al. 2024: Table 4*
Tarapotomys mayoensis	$m_{\%PEc}$*cavio* (Boivin et al. 2024: Table 2)	Wm2	1	129.3	113.0	148.0	34.9	Boivin et al. 2024: Table 4

**Shapajamys pradoi* in Boivin et al. (2024)

Table 3: Description of the dietary categories established in extant caviomorphs and the physical properties of the food elements which compose them following Robinet et al. (2026).

Category	Food items included	Physical properties
fruit-grass	fruits and varied plants (particularly from xeric environment)	tough and hard elements
fruit-insect	fruits and high proportion of insects	varied hard and tough elements
fruit-leaf	fruits and high proportion of dicotyledon leaves and/or fungi	soft and tough elements
fruit-seed	fruits and seeds in high proportions	varied hard elements
grass-leaf	monocotyledon and dicotyledon leaves exclusively or quasi-exclusively	tough, resistant and abrasive
grass-root	subterranean parts of plants in high proportion complemented by leaves of monocotyledon and dicotyledon	hard, abrasive elements
grass-seed	monocotyledon plants and small seeds	abrasive and small hard elements
insect-seed	omnivores, low proportion of leaves, includes insects	varied hard and tough elements
leaf	mainly dicotyledon (shrubs and trees) leaves	tough and abrasive elements
leaf-seed	dicotyledon leaves with the addition of seeds and subterranean plant parts	tough and varied hard elements
young leaf	strong preference for tender leaves, new leaves and sprouts	soft elements

Table 4: Descriptive statistics of dental microwear texture parameters including complexity (no unit), anisotropy (no unit), textural fill volume (µm^3) and heterogeneity of complexity (no unit) for each studied taxon grouped by Shapaja levels in chronological order from older to most recent. Abbreviations: Asfc, complexity; epLsar, anisotropy; HAsfc4, heterogeneity of complexity calculated from 4 subsurfaces; Hasfc9, heterogeneity of complexity calculated from 9 subsurfaces; Hasfc16, heterogeneity of complexity calculated from 16 subsurfaces; N, number of specimens; m, mean; sd, standard deviation; Tfv, textural fill volume.

Taxa	N	Asfc		epLsar x10^3		Tfv		HAsfc4		HAsfc9		HAsfc16	
		m	sd	m	sd	m	sd	m	sd	m	sd	m	sd
TAR20													
cf. *Tarapotomys* sp.	3	0.73	0.18	2.65	1.00	420.58	348.87	0.26	0.15	0.71	0.91	0.55	0.59
lower teeth	1	0.54	NA	3.32	NA	124.51	NA	0.23	NA	0.23	NA	0.24	NA
upper teeth	2	0.83	0.10	2.32	1.16	568.61	334.57	0.28	0.21	0.96	1.15	0.71	0.73
Eoincamys valverdei	1	0.39	NA	3.10	NA	78.86	NA	0.70	NA	0.82	NA	0.77	NA
TAR21													
aff. *Tarapotomys* sp.	1	0.44	NA	4.47	NA	967.06	NA	0.18	NA	0.28	NA	0.31	NA
cf. *Tarapotomys* sp.	1	0.70	NA	2.03	NA	1041.77	NA	0.58	NA	0.57	NA	0.46	NA
Eoincamys parvus	1	2.88	NA	2.77	NA	3918.04	NA	0.14	NA	0.32	NA	0.51	NA
Eoincamys valverdei	4	0.84	0.13	2.74	1.28	513.62	207.20	0.35	0.10	0.41	0.19	0.36	0.12
lower teeth	1	0.81	NA	4.07	NA	568.61	NA	0.32	NA	0.32	NA	0.34	NA
upper teeth	3	0.84	0.15	2.30	1.13	495.29	249.76	0.36	0.13	0.43	0.23	0.37	0.14
Kiskasteiromys raimondii	1	0.98	NA	3.99	NA	1606.23	NA	0.33	NA	0.57	NA	0.55	NA
Tarapotomys subandinus	5	0.90	0.65	3.28	1.31	1081.61	882.94	0.38	0.24	0.39	0.20	0.38	0.21
lower teeth	2	0.52	0.05	4.03	1.42	709.73	493.05	0.47	0.24	0.47	0.13	0.51	0.23
upper teeth	3	1.16	0.77	2.79	1.22	1329.53	1098.69	0.31	0.26	0.33	0.24	0.30	0.18
TAR13													
cf. *Tarapotomys* sp.	1	0.69	NA	5.67	NA	801.04	NA	0.56	NA	0.76	NA	0.56	NA
Eoincamys valverdei	2	0.78	0.10	2.51	0.06	485.60	293.48	0.47	0.06	0.92	0.08	0.86	0.27
TAR22													
Eoincamys parvus	4	0.88	0.32	2.47	0.98	1070.82	734.89	0.46	0.19	0.51	0.32	0.54	0.22
lower teeth	2	0.65	0.32	2.26	0.94	1166.28	1009.58	0.53	0.13	0.70	0.38	0.62	0.21
upper teeth	2	1.11	0.01	2.68	1.35	975.36	751.32	0.40	0.27	0.33	0.13	0.45	0.27
Eoincamys valverdei	1	0.73	NA	1.29	NA	178.47	NA	0.51	NA	0.39	NA	0.47	NA
Selvamys paulus	2	4.54	4.91	4.22	4.74	2380.29	1323.61	0.53	0.58	0.64	0.73	0.55	0.39
TAR01													
Eoincamys cf. *pascuali*	7	0.87	0.46	3.26	2.76	1009.16	1325.92	0.29	0.11	0.35	0.15	0.37	0.13
lower teeth	4	0.78	0.22	3.05	1.88	432.69	201.47	0.32	0.13	0.35	0.15	0.40	0.15
upper teeth	3	0.98	0.74	3.54	4.17	1777.78	1913.76	0.25	0.10	0.34	0.18	0.32	0.10
Mayomys confluens	54	1.21	0.78	3.71	2.10	1155.52	982.68	0.35	0.16	0.47	0.27	0.49	0.28
lower teeth	25	0.99	0.62	3.83	2.15	1099.38	1062.33	0.34	0.15	0.43	0.18	0.45	0.18
upper teeth	29	1.41	0.86	3.61	2.09	1203.92	924.82	0.36	0.17	0.50	0.34	0.53	0.34
Shapajamys labocensis	13	1.01	0.52	2.83	1.56	862.98	649.17	0.29	0.13	0.43	0.22	0.42	0.17
lower teeth	6	0.83	0.32	2.80	1.67	768.53	498.17	0.26	0.14	0.39	0.19	0.36	0.14
upper teeth	7	1.16	0.63	2.85	1.59	943.94	787.06	0.32	0.12	0.47	0.24	0.46	0.20
Tarapotomys mayaensis	18	1.10	0.63	3.72	2.06	1088.35	731.92	0.37	0.20	0.46	0.22	0.50	0.19
lower teeth	6	1.26	0.87	3.59	1.63	970.52	325.55	0.39	0.26	0.50	0.25	0.60	0.22
upper teeth	12	1.02	0.50	3.79	2.31	1147.26	876.57	0.37	0.17	0.44	0.21	0.45	0.16

Table 5: Summary of the results of the post-hoc Wilcoxon paired comparison tests between taxa from the Shapaja section (represented by at least five specimens) and the dietary categories established on extant taxa (following Robinet et al. 2025, in press). When no significant difference is detected, the cell is left empty. Abbreviations: Asfc, complexity; epLsar, anisotropy; Tfv, textural fill volume.

	fruit-grass	fruit-insect	fruit-leaf	fruit-seed	grass-leaf	grass-root	grass-seed	insect-seed	leaf	leaf-seed	young leaf
Eoincamys cf. *pascuali* (TAR-01)	Asfc	Asfc			Asfc	Asfc	Asfc		Asfc		
Mayomys confluens (TAR-01)	Asfc epLsar	Asfc Tfv	Tfv		Asfc epLsar	Asfc epLsar	Asfc epLsar		Asfc		Asfc Tfv
Shapajamys labocensis (TAR-01)	Asfc	Asfc			Asfc	Asfc	Asfc		Asfc		Asfc
Tarapotomys mayoensis (TAR-01)	Asfc	Asfc Tfv	Tfv		Asfc	Asfc	Asfc		Asfc		Asfc Tfv
Tarapotomys subandinus (TAR-21)					Asfc	Asfc	Asfc		Asfc		

Table 6: Summary of the supra-generic systematic classification (Boivin et al. 2019a), crown height category data (based on upper molars; Boivin et al. 2018), results of body mass estimations obtained following equations from Boivin et al. (2024) and results of the DMTA diet estimations for the Shapaja studied taxa.

Taxon	Supra-generic systematic	Crown height category	Body mass	Microwear estimated food property trend	Microwear estimated dietary categories
TAR-20					
E. valverdei	Chinchilloidea	protohypsodont	309.4 g	soft elements	fruit-leaf
cf. *Tarapotomys* sp.	Caviomorpha	brachydont	148.1 g	hard elements	fruit-leaf fruit-seed leaf-seed insect-seed
TAR-21					
E. parvus	Chinchilloidea	mesodont	74.6 g	abrasive elements	leaf
E. valverdei	Chinchilloidea	protohypsodont	168.8 g	hard elements	leaf-seed fruit-leaf
Kichkasteiromys raimondii	Erethizontoidea	brachydont	146.7 g	hard elements	fruit-seed leaf-seed insect-seed leaf
aff. *Tarapotomys* sp.	Caviomorpha	brachydont	100.8 g	soft elements	young leaf fruit-leaf
cf. *Tarapotomys* sp.	Caviomorpha	brachydont	149.3 g	hard elements	fruit-seed leaf-seed insect-seed
Tarapotomys subandinus	Caviomorpha	mesodont	108.9 g	hard elements	fruit-insect fruit-seed insect-seed leaf-seed
TAR-13 & TAR-22					
Eoincamys valverdei - TAR-13	Chinchilloidea	protohypsodont	356.0 g	hard elements	fruit-seed fruit-insect insect-seed
cf. *Tarapotomys* sp. - TAR-13	Caviomorpha	brachydont	382.1 g	hard elements	fruit-leaf fruit-seed
Eoincamys parvus - TAR-22	Chinchilloidea	mesodont	123.6 g	hard elements	fruit-seed leaf-seed fruit-insect insect-seed
E. valverdei - TAR-22	Chinchilloidea	protohypsodont	118.3 g	soft elements	leaf-seed fruit-leaf

Selvamys paulus-TAR-22	Octodontoidea	brachydont	56.1 g	abrasive elements	leaf fruit-grass? grass-seed?
TAR-01					
Eoincamys cf. *pascuali*	Chinchilloidea	brachydont	290.0 g	hard elements	fruit-seed insect-seed leaf-seed
Mayomys confluens	Octochinchilloi	brachydont	133.9 g	hard elements	fruit-seed insect-seed leaf-seed
Shapajamys labocensis	Caviomorpha	brachydont	256.6 g	hard elements	fruit-leaf fruit-seed insect-seed leaf-seed
Tarapotomys mayoensis	Caviomorpha	mesodont	129.3 g	hard elements	fruit-seed insect-seed leaf-seed

Supp. Data 1 - Specimen DMTA parameters

Collection number	Taxon	Locality	Tooth position	File name of the studied surface	Asfc	epLsar x10^{-3}	HAsfc4	HAsfc9	HAsfc16	Tfv
MUSM 2940	aff. *Tarapotomys*	TAR21	U	Zinv-affTsu-MUSM-2940-UMl-hyp-ml.sur	0,44	4,47	0,18	0,28	0,31	967,06
MUSM 2967	cf. *Tarapotomys*	TAR13	L	Zinv-cfTa-MUSM-2967-lm1l-hypd-db.sur	0,69	5,67	0,56	0,76	0,56	801,04
MUSM 3327	cf. *Tarapotomys*	TAR20	L	Zinv-cfTa-MUSM-3327-lm1l-ptcd-db.sur	0,54	3,32	0,23	0,23	0,24	124,51
MUSM 2910	cf. *Tarapotomys*	TAR20	U	Zinv-cfTa-MUSM-2910-UM2r-ptc-ml-bis.sur	0,76	3,13	0,43	1,77	1,23	805,19
MUSM 2911	cf. *Tarapotomys*	TAR20	U	Zinv-cfTa-MUSM-2911-UM3l-ptc-ml.sur	0,90	1,50	0,13	0,14	0,19	332,04
MUSM 2927	cf. *Tarapotomys*	TAR21	L	Zinv-cfTa-MUSM-2927-lm1l-ptcd-db.sur	0,70	2,03	0,58	0,57	0,46	1041,77
MUSM 3292	*Eoincamys* cf. *pascuali*	TAR01	L	Zinv-Ecfpa-MUSM-3292-lm1r-ptcd-db.sur	0,65	4,98	0,26	0,25	0,30	215,82
MUSM 3293	*Eoincamys* cf. *pascuali*	TAR01	L	Zinv-Ecfpa-MUSM-3293-lm2l-ptcd-db.sur	0,85	3,40	0,45	0,54	0,53	348,64
MUSM 3294	*Eoincamys* cf. *pascuali*	TAR01	L	Zinv-Ecfpa-MUSM-3294-lm2l-ptcd-db.sur	0,57	3,34	0,40	0,38	0,54	477,30
MUSM 3296	*Eoincamys* cf. *pascuali*	TAR01	L	Zinv-Ecfpa-MUSM-3296-lm2r-ptcd-db.sur	1,05	0,47	0,17	0,22	0,25	688,98
MUSM 3298	*Eoincamys* cf. *pascuali*	TAR01	U	Zinv-Ecfpa-MUSM-3298-UM1l-ptc-ml.sur	0,63	1,02	0,36	0,54	0,44	103,76
MUSM 3299	*Eoincamys* cf. *pascuali*	TAR01	U	Zinv-Ecfpa-MUSM-3299-UM1l-ptc-ml.sur	0,49	1,25	0,18	0,17	0,27	1365,50
MUSM 3300	*Eoincamys* cf. *pascuali*	TAR01	U	Zinv-Ecfpa-MUSM-3300-UM2r-hyp-ml.sur	1,83	8,35	0,22	0,33	0,26	3864,09
MUSM 2950	*Eoincamys parvus*	TAR21	U	Zinv-Eopa-MUSM-2950-UM1l-ptc-ml.sur	2,88	2,77	0,14	0,32	0,51	3918,04
MUSM E	*Eoincamys parvus*	TAR22	L	Zinv-Eopa-MUSM-E-lm1l-hypd-db.sur	0,43	2,92	0,44	0,43	0,47	452,40
MUSM F	*Eoincamys parvus*	TAR22	L	Zinv-Eopa-MUSM-F-lm3l-ptcd-db.sur	0,88	1,59	0,62	0,97	0,77	1880,16
MUSM 3348	*Eoincamys parvus*	TAR22	U	Zinv-Eopa-MUSM-3348-UMr-hyp-ml.sur	1,10	1,72	0,20	0,23	0,26	444,10
MUSM 3349	*Eoincamys parvus*	TAR22	U	Zinv-Eopa-MUSM-3349-UMl-ptc-ml.sur	1,12	3,63	0,59	0,42	0,64	1506,62
MUSM 2970	*Eoincamys valverdei*	TAR13	U	Zinv-cfEo-MUSM-2970-UMl-hyp-ml.sur	0,71	2,47	0,43	0,86	0,67	693,13
MUSM 2969	*Eoincamys valverdei*	TAR13	U	Zinv-Eova-MUSM-2969-UM3r-ptc-ml.sur	0,85	2,56	0,51	0,98	1,05	278,08
MUSM 3336	*Eoincamys valverdei*	TAR20	U	Zinv-Eova-MUSM-3336-UM1l-ptc-ml.sur	0,39	3,10	0,70	0,82	0,77	78,86
MUSM 2952	*Eoincamys valverdei*	TAR21	L	Zinv-Eova-MUSM-2952-lm1r-ptcd-db.sur	0,81	4,07	0,32	0,32	0,34	568,61
MUSM 2943	*Eoincamys valverdei*	TAR21	U	Zinv-Eova-MUSM-2943-UM2l-ptc-ml.sur	0,78	1,40	0,22	0,21	0,21	473,15
MUSM 2947	*Eoincamys valverdei*	TAR21	U	Zinv-Eova-MUSM-2947-UM1r-ptc-ml.sur	0,73	1,93	0,38	0,44	0,39	257,33
MUSM 2948	*Eoincamys valverdei*	TAR21	U	Zinv-Eova-MUSM-2948-UM1r-ptc-ml.sur	1,02	3,58	0,47	0,66	0,50	755,39
MUSM 3341	*Eoincamys valverdei*	TAR22	U	Zinv-Eova-MUSM-3341-UMl-hyp-ml.sur	0,73	1,29	0,51	0,39	0,47	178,47
MUSM 2925	*Kiskasteiromys raimondii*	TAR21	U	Zinv-Kra-MUSM-2925-UM2r-ptc-ml.sur	0,98	3,99	0,33	0,57	0,55	1606,23
MUSM 3040	*Mayomys confluens*	TAR01	L	Zinv-Mco-MUSM-3040-lm1l-ptcd-db.sur	0,91	7,76	0,37	0,44	0,45	2768,36
MUSM 3041	*Mayomys confluens*	TAR01	L	Zinv-Mco-MUSM-3041-lm1l-ptcd-db.sur	0,57	9,03	0,59	0,78	0,96	53,96
MUSM 3043	*Mayomys confluens*	TAR01	L	Zinv-Mco-MUSM-3043-lm1l-ptcd-db.sur	0,77	3,16	0,36	0,54	0,53	2187,30
MUSM 3044	*Mayomys confluens*	TAR01	L	Zinv-Mco-MUSM-3044-lm1l-ptcd-db.sur	0,71	4,76	0,54	0,67	0,73	610,12
MUSM 3045	*Mayomys confluens*	TAR01	L	Zinv-Mco-MUSM-3045-lm1l-ptcd-db.sur	0,86	5,67	0,35	0,33	0,30	1153,83
MUSM 3046	*Mayomys confluens*	TAR01	L	Zinv-Mco-MUSM-3046-lm1l-ptcd-db-bis.sur	1,28	5,27	0,39	0,44	0,41	390,14
MUSM 3047	*Mayomys confluens*	TAR01	L	Zinv-Mco-MUSM-3047-lm1l-ptcd-db.sur	0,65	3,33	0,30	0,82	0,78	734,63
MUSM 3048	*Mayomys confluens*	TAR01	L	Zinv-Mco-MUSM-3048-lm1l-ptcd-db.sur	1,19	1,10	0,30	0,44	0,36	502,21
MUSM 3050	*Mayomys confluens*	TAR01	L	Zinv-Mco-MUSM-3050-lm1l-ptcd-db.sur	1,48	3,20	0,49	0,50	0,47	3382,63
MUSM 3054	*Mayomys confluens*	TAR01	L	Zinv-Mco-MUSM-3054-lm1l-ptcd-db.sur	0,60	2,83	0,25	0,21	0,23	174,32
MUSM 3063	*Mayomys confluens*	TAR01	L	Zinv-Mco-MUSM-3063-lm1r-hypd-db.sur	0,94	4,08	0,20	0,40	0,51	630,87
MUSM 3066	*Mayomys confluens*	TAR01	L	Zinv-Mco-MUSM-3066-lm1r-ptcd-db.sur	0,50	1,43	0,41	0,45	0,47	112,06
MUSM 3074	*Mayomys confluens*	TAR01	L	Zinv-Mco-MUSM-3074-lm2l-ptcd-db.sur	0,71	4,44	0,30	0,47	0,46	1041,77
MUSM 3075	*Mayomys confluens*	TAR01	L	Zinv-Mco-MUSM-3075-lm2l-ptcd-db.sur	0,47	5,14	0,11	0,15	0,19	16,60
MUSM 3076	*Mayomys confluens*	TAR01	L	Zinv-Mco-MUSM-3076-lm2l-ptcd-db.sur	2,60	3,78	0,36	0,55	0,55	2249,55
MUSM 3078	*Mayomys confluens*	TAR01	L	Zinv-Mco-MUSM-3078-lm2l-ptcd-db.sur	0,50	3,52	0,43	0,71	0,47	16,60
MUSM 3081	*Mayomys confluens*	TAR01	L	Zinv-Mco-MUSM-3081-lm2l-ptcd-db.sur	0,71	1,91	0,23	0,46	0,59	149,42
MUSM 3084	*Mayomys confluens*	TAR01	L	Zinv-Mco-MUSM-3084-lm2l-ptcd-db.sur	1,34	0,98	0,18	0,20	0,32	1382,11
MUSM 3085	*Mayomys confluens*	TAR01	L	Zinv-Mco-MUSM-3085-lm2l-ptcd-db.sur	0,99	3,18	0,30	0,26	0,29	701,43
MUSM 3087	*Mayomys confluens*	TAR01	L	Zinv-Mco-MUSM-3087-lm2l-hypd-db.sur	0,99	4,39	0,21	0,18	0,26	676,53
MUSM 3088	*Mayomys confluens*	TAR01	L	Zinv-Mco-MUSM-3088-lm2l-ptcd-db.sur	0,48	2,95	0,76	0,25	0,22	987,81
MUSM 3091	*Mayomys confluens*	TAR01	L	Zinv-Mco-MUSM-3091-lm2r-hypd-db.sur	0,78	2,11	0,46	0,41	0,38	1419,46
MUSM 3092	*Mayomys confluens*	TAR01	L	Zinv-Mco-MUSM-3092-lm2r-ptcd-db.sur	1,06	7,83	0,25	0,49	0,54	2071,08
MUSM 3093	*Mayomys confluens*	TAR01	L	Zinv-Mco-MUSM-3093-lm2r-ptcd-db.sur	0,55	3,46	0,21	0,34	0,34	344,49
MUSM 3095	*Mayomys confluens*	TAR01	L	Zinv-Mco-MUSM-3095-lm2r-hypd-db.sur	2,99	0,43	0,08	0,37	0,34	3727,12
MUSM 3169	*Mayomys confluens*	TAR01	U	Zinv-Mco-MUSM-3169-UM1l-hyp-ml.sur	2,83	3,69	0,68	1,61	1,69	1294,95
MUSM 3170	*Mayomys confluens*	TAR01	U	Zinv-Mco-MUSM-3170-UM1l-ptc-ml.sur	0,69	2,01	0,23	0,24	0,32	485,60
MUSM 3173	*Mayomys confluens*	TAR01	U	Zinv-Mco-MUSM-3173-UM1r-ptc-ml.sur	0,36	1,69	0,31	0,96	0,79	913,10
MUSM 3174	*Mayomys confluens*	TAR01	U	Zinv-Mco-MUSM-3174-UM1r-ptc-ml.sur	1,29	5,81	0,93	1,12	1,39	1855,26
MUSM 3175	*Mayomys confluens*	TAR01	U	Zinv-Mco-MUSM-3175-UM1r-hyp-ml.sur	0,97	2,44	0,40	0,31	0,38	1062,52
MUSM 3178	*Mayomys confluens*	TAR01	U	Zinv-Mco-MUSM-3178-UM1r-ptc-ml.sur	2,76	0,88	0,35	0,54	0,46	1743,20
MUSM 3179	*Mayomys confluens*	TAR01	U	Zinv-Mco-MUSM-3179-UM1r-hyp-ml.sur	3,83	3,45	0,50	0,92	0,95	767,84
MUSM 3180	*Mayomys confluens*	TAR01	U	Zinv-Mco-MUSM-3180-UM1r-ptc-ml.sur	0,55	0,90	0,42	0,35	0,34	261,48
MUSM 3184	*Mayomys confluens*	TAR01	U	Zinv-Mco-MUSM-3184-UM2l-hyp-ml.sur	2,24	3,89	0,20	0,25	0,31	1178,73
MUSM 3185	*Mayomys confluens*	TAR01	U	Zinv-Mco-MUSM-3185-UM2l-hyp-ml.sur	1,47	7,61	0,32	0,30	0,30	1054,22
MUSM 3189	*Mayomys confluens*	TAR01	U	Zinv-Mco-MUSM-3189-UM2l-ptc-ml.sur	0,87	5,12	0,24	0,31	0,36	402,60
MUSM 3191	*Mayomys confluens*	TAR01	U	Zinv-Mco-MUSM-3191-UM2l-hyp-ml.sur	1,01	6,10	0,37	0,52	0,58	2125,04
MUSM 3257	*Mayomys confluens*	TAR01	U	Zinv-Mco-MUSM-3257-UM2r-ptc-ml.sur	0,93	2,50	0,33	0,31	0,38	1656,04
MUSM 3258	*Mayomys confluens*	TAR01	U	Zinv-Mco-MUSM-3258-UM2r-hyp-ml.sur	0,89	3,22	0,30	0,30	0,28	552,01
MUSM 3260	*Mayomys confluens*	TAR01	U	Zinv-Mco-MUSM-3260-UM2r-ptc-ml.sur	1,19	1,90	0,31	0,47	0,44	257,33
MUSM 3261	*Mayomys confluens*	TAR01	U	Zinv-Mco-MUSM-3261-UM2r-hyp-ml.sur	0,90	5,67	0,58	0,83	0,69	1697,54
MUSM 3264	*Mayomys confluens*	TAR01	U	Zinv-Mco-MUSM-3264-UM3l-ptc-ml.sur	0,86	2,42	0,31	0,81	0,72	1253,44
MUSM 3268	*Mayomys confluens*	TAR01	U	Zinv-Mco-MUSM-3268-UM3l-ptc-ml.sur	0,38	3,87	0,43	0,58	0,41	531,26
MUSM 3272	*Mayomys confluens*	TAR01	U	Zinv-Mco-MUSM-3272-UM3l-ptc-ml.sur	2,71	2,61	0,26	0,36	0,49	896,50
MUSM 3273	*Mayomys confluens*	TAR01	U	Zinv-Mco-MUSM-3273-UM3l-ptc-ml.sur	0,64	7,61	0,28	0,52	0,56	830,09
MUSM 3276	*Mayomys confluens*	TAR01	U	Zinv-Mco-MUSM-3276-UM3r-ptc-ml.sur	2,66	4,66	0,27	0,38	0,52	2071,08
MUSM 3278	*Mayomys confluens*	TAR01	U	Zinv-Mco-MUSM-3278-UM3r-ptc-ml.sur	1,46	2,84	0,18	0,15	0,24	722,18
MUSM 3281	*Mayomys confluens*	TAR01	U	Zinv-Mco-MUSM-3281-UM3r-ptc-ml.sur	2,20	0,36	0,25	0,23	0,32	1178,73
MUSM 3288	*Mayomys confluens*	TAR01	U	Zinv-Mco-MUSM-3288-UM3r-ptc-ml.sur	0,96	6,45	0,57	0,39	0,50	933,86
MUSM A	*Mayomys confluens*	TAR01	U	Zinv-Mco-MUSM-A-UMl-ptc-ml.sur	1,37	1,80	0,54	0,81	0,67	1066,67

Supp. Data 1 - Specimen DMTA parameters

Collection number	Taxon	Locality	Tooth position	File name of the studied surface	Asfc	epLsar x10^{-3}	HAsfc4	HAsfc9	HAsfc16	Tfv
MUSM E	*Mayomys confluens*	TAR01	U	Zinv-Mco-MUSM-E-UMl-ptc-ml.sur	1,07	6,10	0,35	0,28	0,32	415,05
MUSM G	*Mayomys confluens*	TAR01	U	Zinv-Mco-MUSM-G-UMl-ptc-ml.sur	1,60	1,47	0,19	0,21	0,27	1456,81
MUSM M	*Mayomys confluens*	TAR01	U	Zinv-Mco-MUSM-M-UMr-hyp-ml.sur	0,74	1,67	0,18	0,18	0,15	1074,97
MUSM O	*Mayomys confluens*	TAR01	U	Zinv-Mco-MUSM-O-UMr-hyp-ml.sur	1,36	6,02	0,25	0,38	0,60	5175,64
MUSM 2960	*Selvamys paulus*	TAR22	U	Zinv-Sepa-MUSM-2960-UM2r-ptc-ml.sur	8,01	0,86	0,12	0,13	0,28	3316,23
MUSM 3340	*Selvamys paulus*	TAR22	U	Zinv-Sepa-MUSM-3340-UM2r-ptc-ml.sur	1,06	7,57	0,94	1,16	0,83	1444,36
MUSM 2973	*Shapajamys labocensis*	TAR01	L	Zinv-Sha-MUSM-2973-lm1l-ptcd-db.sur	1,04	1,93	0,26	0,52	0,37	1253,44
MUSM 2974	*Shapajamys labocensis*	TAR01	L	Zinv-Sha-MUSM-2974-lm1r-ptcd-db.sur	1,17	2,63	0,52	0,60	0,61	1133,08
MUSM 2975	*Shapajamys labocensis*	TAR01	L	Zinv-Sha-MUSM-2975-lm1r-ptcd-db.sur	0,59	1,63	0,14	0,20	0,23	311,29
MUSM 2979	*Shapajamys labocensis*	TAR01	L	Zinv-Sha-MUSM-2979-lm2r-ptcd-db.sur	0,51	1,04	0,11	0,19	0,25	153,57
MUSM 2981	*Shapajamys labocensis*	TAR01	L	Zinv-Sha-MUSM-2981-lm2l-ptcd-db.sur	1,14	4,14	0,25	0,25	0,36	1240,99
MUSM 3341	*Shapajamys labocensis*	TAR01	L	Zinv-Sha-MUSM-3341-lml-ptcd-db.sur	0,52	5,43	0,28	0,56	0,36	518,81
MUSM 2987	*Shapajamys labocensis*	TAR01	U	Zinv-Sha-MUSM-2987-UMr-hyp-ml-bis.sur	1,83	5,97	0,24	0,29	0,24	1353,05
MUSM 2989	*Shapajamys labocensis*	TAR01	U	Zinv-Sha-MUSM-2989-UMr-hyp-ml.sur	0,76	3,24	0,22	0,23	0,34	153,57
MUSM 2990	*Shapajamys labocensis*	TAR01	U	Zinv-Sha-MUSM-2990-UMr-hyp-ml.sur	0,67	2,16	0,55	0,73	0,57	543,71
MUSM 2991	*Shapajamys labocensis*	TAR01	U	Zinv-Sha-MUSM-2991-UMr-ptc-ml.sur	0,77	1,54	0,24	0,43	0,47	676,53
MUSM 2992	*Shapajamys labocensis*	TAR01	U	Zinv-Sha-MUSM-2992-UMr-ptc-ml.sur	0,49	1,08	0,44	0,42	0,37	70,56
MUSM 2994	*Shapajamys labocensis*	TAR01	U	Zinv-Sha-MUSM-2994-UM1l-ptc-ml.sur	2,04	3,07	0,27	0,88	0,85	2108,44
MUSM 2996	*Shapajamys labocensis*	TAR01	U	Zinv-Sha-MUSM-2996-UMr-hyp-ml-.sur	1,58	2,89	0,29	0,34	0,39	1701,69
MUSM 3304	*Tarapotomys mayoensis*	TAR01	L	Zinv-Tma-MUSM-3304-lm1l-ptcd-db.sur	2,88	2,55	0,04	0,46	0,40	1390,41
MUSM 3306	*Tarapotomys mayoensis*	TAR01	L	Zinv-Tma-MUSM-3306-lm1r-hypd-db.sur	1,45	3,45	0,23	0,21	0,27	867,45
MUSM 3309	*Tarapotomys mayoensis*	TAR01	L	Zinv-Tma-MUSM-3309-lm2l-ptcd-db.sur	1,08	2,00	0,67	0,49	0,70	1199,49
MUSM 3310	*Tarapotomys mayoensis*	TAR01	L	Zinv-Tma-MUSM-3310-lm2r-hypd-db.sur	0,60	3,14	0,70	0,94	0,80	792,74
MUSM 3311	*Tarapotomys mayoensis*	TAR01	L	Zinv-Tma-MUSM-3311-lm2r-ptcd-db.sur	0,47	3,73	0,24	0,58	0,64	477,30
MUSM 3312	*Tarapotomys mayoensis*	TAR01	L	Zinv-Tma-MUSM-3312-lm2r-ptcd-db.sur	1,09	6,67	0,44	0,33	0,78	1095,72
MUSM 3323	*Tarapotomys mayoensis*	TAR01	U	Zinv-Tma-MUSM-3323-UM1l-ptc-ml.sur	1,97	1,56	0,49	0,76	0,71	1452,66
MUSM 3326	*Tarapotomys mayoensis*	TAR01	U	Zinv-Tma-MUSM-3326-UM1r-ptc-ml.sur	1,93	5,37	0,31	0,42	0,49	1863,56
MUSM 3329	*Tarapotomys mayoensis*	TAR01	U	Zinv-Tma-MUSM-3329-UM2l-ptc-ml.sur	0,79	6,17	0,57	0,71	0,62	742,93
MUSM 3330	*Tarapotomys mayoensis*	TAR01	U	Zinv-Tma-MUSM-3330-UM2l-hyp-ml.sur	0,94	1,51	0,31	0,23	0,34	2913,63
MUSM 3331	*Tarapotomys mayoensis*	TAR01	U	Zinv-Tma-MUSM-3331-UM2l-ptc-ml.sur	0,97	2,48	0,60	0,62	0,56	618,42
MUSM 3332	*Tarapotomys mayoensis*	TAR01	U	Zinv-Tma-MUSM-3332-UM2r-ptc-ml.sur	1,21	5,09	0,26	0,72	0,33	1539,82
MUSM 3333	*Tarapotomys mayoensis*	TAR01	U	Zinv-Tma-MUSM-3333-UM2r-ptc-ml.sur	0,83	5,81	0,55	0,32	0,50	2291,06
MUSM 3334	*Tarapotomys mayoensis*	TAR01	U	Zinv-Tma-MUSM-3334-UM3l-ptc-ml.sur	1,07	1,88	0,33	0,45	0,65	859,15
MUSM 3335	*Tarapotomys mayoensis*	TAR01	U	Zinv-Tma-MUSM-3335-UM3r-ptc-ml.sur	0,75	7,31	0,32	0,33	0,41	41,50
MUSM 3337	*Tarapotomys mayoensis*	TAR01	U	Zinv-Tma-MUSM-3337-UM3r-ptc-ml.sur	0,37	0,77	0,04	0,15	0,16	166,02
MUSM 3338	*Tarapotomys mayoensis*	TAR01	U	Zinv-Tma-MUSM-3338-UM3r-hyp-ml.sur	0,39	1,79	0,19	0,21	0,30	506,36
MUSM 3367	*Tarapotomys mayoensis*	TAR01	U	Zinv-Tma-MUSM-3367-UM1r-hyp-ml.sur	1,01	5,71	0,40	0,42	0,39	771,99
MUSM 2930	*Tarapotomys subandinus*	TAR21	L	Zinv-Tsu-MUSM-2930-lm2r-ptcd-db.sur	0,56	3,03	0,30	0,38	0,35	361,09
MUSM 2931	*Tarapotomys subandinus*	TAR21	L	Zinv-Tsu-MUSM-2931-lm3r-ptcd-db.sur	0,48	5,03	0,63	0,57	0,67	1058,37
MUSM 2933	*Tarapotomys subandinus*	TAR21	U	Zinv-Tsu-MUSM-2933-UDP4r-ptc-ml.sur	1,98	2,07	0,12	0,17	0,13	257,33
MUSM 2934	*Tarapotomys subandinus*	TAR21	U	Zinv-Tsu-MUSM-2934-UP4r-hyp-ml.sur	0,45	4,20	0,21	0,22	0,27	1278,34
MUSM 2939	*Tarapotomys subandinus*	TAR21	U	Zinv-Tsu-MUSM-2939-UM2r-hyp-ml.sur	1,05	2,10	0,61	0,60	0,49	2452,93

Supp. Data 2 - Body mass estimates

Taxa	Mass inf cor (g)	Mass sup cor (g)	Interval amplitude
TAR-20			
Eoincamys valverdei	132.497	722.687	590.191
cf. *Tarapotomys*	109.016	201.080	92.065
TAR-21			
Eoincamys parvus	43.023	129.336	86.313
Eoincamys valverdei	119.873	237.786	117.913
Kichkasteiromys raimondii	107.941	199.390	91.449
aff. *Tarapotomys*	73.437	138.476	65.039
cf. *Tarapotomys*	109.878	202.867	92.990
Tarapotomys subandinus	81.650	145.334	63.684
TAR-13			
Eoincamys valverdei	237.694	533.026	295.332
cf. *Tarapotomys*	274.845	531.057	256.213
TAR-22			
Eoincamys parvus	79.978	191.093	111.115
Eoincamys valverdei	76.690	182.511	105.820
Selvamys paulus	36.590	85.918	49.328
TAR-01			
Eoincamys cf. *pascuali*	205.383	409.587	204.204
Mayomys confluens	99.168	180.794	81.626
Shapajamys labocensis	183.003	359.803	176.800
Tarapotomys mayoensis	95.964	174.247	78.283

Supp. Data 3 - Statistical analyses between extinct taxa from the Shapaja section

Supplementary table 1: Results of the ANOVA for each parameter[a] of dental microwear texture Box-Cox transformed between taxa from the Shapaja section represented by at least five specimens. Abbreviation: d.f., degree of freedom.

	d.f.	Sum of Squares	Mean Squares	F value	p value
Asfc					
Taxon	4	0.845	0.211	0.710	0.587
Residuals	92	27.377	0.298		
epLsar					
Taxon	6	0.009	0.002	0.551	0.699
Residuals	98	0.362	0.004		
HAsfc4					
Taxon	6	0.171	0.426	0.480	0.750
Residuals	98	8.170	0.089		
HAsfc9					
Taxon	6	0.545	0.136	0.506	0.732
Residuals	98	24.804	0.270		
HAsfc16					
Taxon	6	0.935	0.234	1.075	0.374
Residuals	98	19.991	0.217		
Tfv					
Taxon	6	125.800	31.448	0.355	0.840
Residuals	98	8140.500	88.484		

[a]Asfc: complexity; epLsar: anisotropy; HAsfc: heterogeneity of complexity calculated from 4, 9 and 16 subsurfaces, respectively; Tfv: textural fill volume.